



HAL
open science

Reference Energies for Valence Ionizations and Satellite Transitions

Antoine Marie, Pierre-François Loos

► **To cite this version:**

Antoine Marie, Pierre-François Loos. Reference Energies for Valence Ionizations and Satellite Transitions. *Journal of Chemical Theory and Computation*, 2024, 20 (11), pp.4751-4777. 10.1021/acs.jctc.4c00216 . hal-04472287

HAL Id: hal-04472287

<https://hal.science/hal-04472287>

Submitted on 22 Feb 2024

HAL is a multi-disciplinary open access archive for the deposit and dissemination of scientific research documents, whether they are published or not. The documents may come from teaching and research institutions in France or abroad, or from public or private research centers.

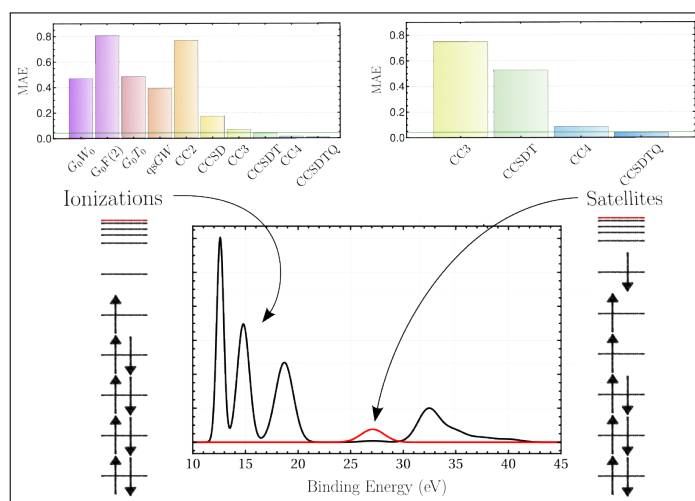
L'archive ouverte pluridisciplinaire **HAL**, est destinée au dépôt et à la diffusion de documents scientifiques de niveau recherche, publiés ou non, émanant des établissements d'enseignement et de recherche français ou étrangers, des laboratoires publics ou privés.

Reference Energies for Valence Ionizations and Satellite Transitions

Antoine Marie^{1, a)} and Pierre-François Loos^{1, b)}

Laboratoire de Chimie et Physique Quantiques (UMR 5626), Université de Toulouse, CNRS, UPS, France

Upon ionization of an atom or a molecule, another electron (or more) can be simultaneously excited. These concurrently generated states are called “satellites” (or shake-up transitions) as they appear in ionization spectra as higher-energy peaks with weaker intensity and larger width than the main peaks associated with single-particle ionizations. Satellites, which correspond to electronically excited states of the cationic species, are notoriously challenging to model using conventional single-reference methods due to their high excitation degree compared to the neutral reference state. This work reports 40 satellite transition energies and 58 valence ionization potentials of full configuration interaction (FCI) quality computed in small molecular systems. Following the protocol developed for the QUEST database [Véril, M.; et al. *Wiley Interdiscip. Rev.: Comput. Mol. Sci.* **2021**, *11*, e1517], these reference energies are computed using the configuration interaction using a perturbative selection made iteratively (CIPSI) method. In addition, the accuracy of the well-known coupled-cluster (CC) hierarchy (CC2, CCSD, CC3, CCSDT, CC4, and CCSDTQ) is gauged against these new accurate references. The performances of various approximations based on many-body Green’s functions (*GW*, *GF2*, and *T*-matrix) for ionization potentials are also analyzed. Their limitations in correctly modeling satellite transitions are discussed.



I. INTRODUCTION

Ionization spectra, probed through techniques like UV-Vis, X-ray, synchrotron radiation, or electron impact spectroscopy, are invaluable tools in experimental chemistry for unraveling the structural intricacies of atoms, molecules, clusters, or solids.^{1–3} Through the positions and intensities of their peaks, these spectra offer key information about the sampled system. For example, these measurements can be realized in various phases (gas, liquid, or solid) and, hence, analyzed to understand changes in electronic structure in these different phases.^{4–7}

Typically, within the energy range from 10 eV to 40 eV, valence-shell ionization occurs, while the core shell is probed at significantly higher energies.⁸ This higher-energy region is not considered in the present study but

the concepts that we discuss below in the context of valence-shell spectra are also encountered in the case of core electron spectroscopy. Particularly, between 10 eV and 20 eV, ionization spectra of small molecules usually exhibit well-defined peaks. These sharp and intense ionization peaks are essentially single-particle processes, *i.e.*, an electron is ejected from the molecule and measured by the detector. These first peaks are associated with outer-valence orbitals. At slightly higher energies, typically several eV, the situation is more complex as, in addition to inner-valence single-particle ionization peaks, additional broader and less intense peaks appear. These are referred to as satellites or shake-up transitions.

In molecules, satellites represent ionization events coupled with the simultaneous excitation of one or more electrons. They are thus intrinsically many-body phenomena, as one must describe at least two electrons and one hole. Satellite transitions can be seen as the equivalent of double excitations in the realm of neutral excitations. Because one must describe processes involving two electrons and two holes, double excitations pose significant

^{a)}Electronic mail: amarie@irsamc.ups-tlse.fr

^{b)}Electronic mail: loos@irsamc.ups-tlse.fr

challenges for theoretical methods,^{9–11} and the same holds true for satellite transitions. Consequently, such states can hardly be described by mean-field formalisms, such as Hartree-Fock (HF) theory. Thus, properly accounting for correlation effects is crucial to describe satellite transitions.¹² In particular, a recent study has emphasized the dynamic nature of this correlation.¹³ In the following the term “ionization” is employed to refer to single-particle processes, also called Koopmans’ states.

Theoretical benchmarks play a pivotal role in evaluating the accuracy of approximation methods.^{14–23} Concerning principal ionization potentials (IPs), which correspond to an electron detachment from the highest-occupied molecular orbital, two prominent benchmark sets are widely recognized: the extensively used *GW*100 test set^{24–26} and a set comprising 24 organic acceptor molecules.^{27–30} Both sets rely on reference values obtained from coupled-cluster (CC) with singles, doubles, and perturbative triples [CCSD(T)] calculations^{31–33} and determined by the energy difference between the neutral and cationic ground-state energies.³⁴ Recently, Ranasinghe *et al.* created a comprehensive benchmark set including not only principal IPs but also outer- and inner-valence IPs of organic molecules.³⁵ Reference values for this set were computed using the IP version of the equation-of-motion (IP-EOM) formalism^{36–40} of CC theory with up to quadruple excitations (IP-EOM-CCSDTQ) for the smallest molecules.³⁵ Note that these benchmarks and the present work deal with vertical IPs, and we shall not address their adiabatic counterparts here.

To demonstrate its predictive capability for valence ionization spectra, an electronic structure method must precisely locate the positions of both outer- and inner-valence ionization potentials, along with valence satellites. However, to the best of our knowledge, no established theoretical benchmarks exist for satellite energies in molecules. Consequently, the primary goal of this manuscript is to establish such a set of values. Finally, it is important to mention that to be fully predictive a method should be able to predict the intensities associated with of these transitions. However, benchmarking intensities is beyond the scope of this work and will be considered in a future study.

Nowadays, a plethora of methods exist to compute IPs in molecular systems. The most straightforward among them is HF where occupied orbital energies serve as approximations of the IPs (up to a minus sign) by virtue of Koopmans’ theorem.⁴¹ Similarly, within density-functional theory (DFT), the Kohn-Sham (KS) orbital energies can be used as approximate ionization energies.^{42–44} The accurate computation of IPs within KS-DFT is still an ongoing research field with, for example, long-range corrected functionals,⁴⁵ KS potential adjusters,^{46,47} double-hybrids functionals,⁴⁸ or even functionals directly optimized for IPs.^{35,49–51} An alternative way to compute electron detachment energies at the HF or KS-DFT levels is through the state-specific self-consistent-field (Δ SCF) formalism, where one optimizes both the neutral ground

state and the cationic state of interest, the IPs being computed as the difference between these two total energies. This strategy has been mainly used to compute core binding energies and is known to perform better than Koopmans’ theorem thanks to orbital relaxation.^{52–58}

Mean-field methods, such as HF and KS-DFT, provide a first approximation to IPs but greater accuracy is often required. The well-known configuration interaction (CI) and CC formalisms provide two systematically improvable paths toward the exact IPs.^{38–40,59} Within both frameworks, IPs can be obtained through a diagonalization of a given Hamiltonian matrix in the $(N - 1)$ -electron sector of the Fock space or through a state-specific formalism similar to Δ SCF. Ranasinghe *et al.* have shown that the mean absolute error (MAE) of IP-EOM-CCSDT with respect to CCSDTQ is only 0.03 eV for a set containing 42 IPs of small molecules.³⁵ Considering the same set, the cheaper IP-EOM-CCSD method has a MAE of 0.2 eV. Recently, the unitary CC formalism has also been employed within the IP-EOM formalism to compute IPs.⁶⁰ As mentioned above, the Δ SCF strategy can be extended to correlated methods which leads to the Δ CC method as an alternative to obtain IPs.⁶¹ Once again, it has been mainly used to compute core IPs but it is also possible to determine valence IPs.^{62–64} Selected CI (SCI)^{65–68} provides yet another systematically improvable formalism for IPs. Indeed, by increasing progressively the number of determinants included in the variational space, one can in principle reach any desired accuracy, up to the full CI (FCI) limit.^{69–75} Recently, the adaptive sampling CI algorithm^{72,76–78} has been used to compute accurate valence ionization spectra of small molecules.¹³

In contrast to the wave function methods previously mentioned, one can also compute IPs via a more natural way based on electron propagators (or Green’s functions), such as the *GW* approximation^{79–81} or the algebraic diagrammatic construction (ADC).^{82,83} The *GW* methodology has a myriad of variants. Its one-shot G_0W_0 version,^{84–90} which was first popularized in condensed matter physics, is now routinely employed to compute IPs of molecular systems and can be applied to systems with thousands of correlated electrons.^{91–103} Other flavors of *GW* such as eigenvalue-only self-consistent *GW* (ev*GW*)^{104–108} and quasi-particle self-consistent *GW* (qs*GW*)^{108–113} have also been benchmarked for IPs. Although the *GW* method is by far the most popular approach nowadays, there exist some alternatives, such as the second Born [also known as second-order Green’s function (GF2) in the quantum chemistry community]^{41,114–129} or the *T*-matrix^{130–147} approximations. However, none of them has enjoyed the popularity and performances reached by *GW*.^{148–150} On the darker side, one of the main flaws of the *GW* approximation is its lack of systematic improvability, especially compared to the wave function methods mentioned above. Various beyond-*GW* schemes have been designed and gauged, but none of them seem to offer, at a reasonable cost, a systematic route toward exact IPs.^{131,132,137,151–168}

The prediction of satellite peaks in molecules garnered attention in the late 20th century. In the 70’s, Schirmer and coworkers applied extensively the 2ph-TDA [and the closely related ADC(3)] formalism to study the inner-valence region of small molecules.^{12,169–181} CI methods were also employed by other groups to study this energetic region.^{182–193} In both formalisms, the satellite energies are easily accessible as they correspond to higher-energy roots of the ADC and CI matrices. After relative successes for outer-valence ionizations, it was quickly realized that the inner-valence shell is much more difficult to describe due to the overlap between the inner-valence ionization and the outer-valence satellite peaks.¹⁷³ As mentioned above, the satellites present in this energy range cannot be described without taking into account electron correlation at a high level of theory. Even more troublesome, in some cases, the orbital picture (or quasiparticle approximation) completely breaks down. In other words, it becomes meaningless to assign the character of ionization or satellite to a given transition.^{169,173} In the following decades, the symmetry-adapted-cluster (SAC) CI was extensively used to study the inner-valence ionization spectra of small organic molecules.^{194–205} SAC-CI was shown to be able to compute satellite energies in quantitative agreement with experiments while methods based on Green’s functions have been in qualitative agreement, at best.

Satellites, sometimes called sidebands, have been extensively studied in the context of materials.⁷⁹ These additional peaks, which can have different natures, are observed in photoemission spectra of metals, semiconductors, and insulators.^{206–215} In “simple” metals, such as bulk sodium^{206,213} or its paradigmatic version, the uniform electron gas,^{25,214,216–221} satellites are usually created by the strong coupling between electrons and plasmon excitations. It is widely recognized that *GW* does not properly describe satellite structures in solids, and it is required to include vertex corrections to describe these many-body effects. One of the most common schemes to study satellites in solids is the cumulant expansion,^{210,219,222–224} which is formally linked to electron-boson Hamiltonians.^{156,225–227}

Nowadays, computational and theoretical progress allows us to systematically converge to exact neutral excitation energies of small molecules,^{10,73,228–231} and this holds as well for charged excitations like IPs. For example, Olsen *et al.* computed the exact first three IPs of water using FCI,⁵⁹ while Kamiya and Hirata went up to IP-EOM-CCSDTQ to compute highly accurate satellite energies for CO and N₂.³⁹ As mentioned previously, a set of 42 IPs of CCSDTQ quality is also available now.³⁵ Finally, Chatterjee and Sokolov recently computed 27 valence IPs using the semistochastic heatbath SCI method^{73,232,233} in order to benchmark their multi-reference implementation of ADC.^{234,235} They also report FCI-quality energies for the four lowest satellite states of the carbon dimer. The present manuscript contributes to this line of research by providing 40 satellite energies of FCI quality. Additionally, 58 valence IPs are reported as well, among which 37 were not present in Chatterjee’s CCSDTQ nor

Sokolov’s FCI benchmark set.³⁵ This study is part of a larger database of highly accurate vertical neutral excitation energies named QUEST which now includes more than 900 excitation energies.^{23,230,231,236–243} Our hope is that these new data will serve as a valuable resource for encouraging the development of novel approximate methods dedicated to computing satellite energies, building on the success of benchmarks with highly-accurate reference energies and properties.

II. COMPUTATIONAL DETAILS

The geometries of the molecular systems considered here have been optimized using CFOUR²⁴⁴ following QUEST’s protocol,^{23,238} *i.e.* at the CC3/aug-cc-pVTZ level^{245,246} without frozen-core approximation. The corresponding cartesian coordinates can be found in the [Supporting Information](#). Throughout the paper the basis sets considered are Pople’s 6-31+G*^{247–253} and Dunning’s aug-cc-pVXZ (where X = D, T, and Q).^{254–257}

A. Selected CI calculations

All SCI calculations have been performed using the configuration interaction using a perturbative selection made iteratively (CIPSI) algorithm^{67,228,258–261} as implemented in QUANTUM PACKAGE.²⁶² For more details about the CIPSI method and its implementation, see Ref. 262. The frozen-core approximation has been enforced in all calculations using the conventions of GAUSSIAN16²⁶³ and CFOUR,²⁴⁴ except for Li and Be where the 1s orbital was not frozen.

We followed a two-step procedure to obtain the ionization and satellite energies, I_ν^N , at the SCI level. First, two single-state calculations are performed for the N - and $(N - 1)$ -electron ground states. This yields the principal IP of the system, $I_0^N = E_0^{N-1} - E_0^N$, where E_0^{N-1} and E_0^N are the ground-state energies of the N - and $(N - 1)$ -electron systems, respectively. Then, a third, multi-state calculation is performed to compute the neutral excitation energies of the $(N - 1)$ -electron system, $\Delta E_\nu^{N-1} = E_\nu^{N-1} - E_0^N$, where E_ν^{N-1} is the energy of the ν th excited states associated with the $(N - 1)$ -electron system. Combining these three calculations, one gets

$$I_\nu^N = E_0^{N-1} - E_0^N + \Delta E_\nu^{N-1} \quad (1)$$

Because single-state calculations converge faster than their multi-state counterparts, the limiting factor associated with the present CIPSI calculations are the convergence of the excitation energies ΔE_ν^{N-1} , and this is what determines ultimately the overall accuracy of I_ν^N .

For each system and state, the SCI variational energy has been extrapolated as a function of the second-order perturbative correction using a linear weighted fit using the last 3 to 6 CIPSI iterations.^{73,74,264,265} The weights

have been taken as the square of the inverse of the perturbative correction. The estimated FCI energy is then chosen amongst these extrapolated values obtained with a variable number of points such that the standard error associated with the extrapolated energy is minimal. Below, we report error bars associated with these extrapolated FCI values. However, it is worth remembering that these do not correspond to genuine statistical errors. The fitting procedure has been performed with MATHEMATICA using default settings.²⁶⁶

B. Coupled-cluster calculations

The EOM-CC calculations have been done using CFOUR with the default convergence thresholds.²⁴⁴ Again, the frozen-core approximation was enforced systematically. IP-EOM-CC calculations, *i.e.*, diagonalization of the CC effective Hamiltonian in the $(N - 1)$ -electron sector of the Fock space,^{36–40} have been performed for CCSD,^{32,36,267–270} CCSDT,^{37,271–273} and CCSDTQ.^{274–278} At the CCSD level, the EOM space includes the one-hole (1h) and the two-hole-one-particle (2h1p) configurations, while the three-hole-two-particle (3h2p) and four-hole-three-particle (4h3p) configurations are further added at the CCSDT and CCSDTQ, respectively. Note that, within the CC formalism, we assume that the IP and electron affinity (EA) sectors are decoupled.^{279–282} For CC2,^{283,284} CC3,^{245,246,285–287} and CC4,^{240,288–290} diagonalization in the $(N - 1)$ -electron sector of the Fock space is not available yet. Hence, it has been carried out in the N -electron sector of the Fock space^{36,37,291–295} with an additional very diffuse (or bath) orbital with zero energy to obtain ionization and satellite energies. Therefore, at the CC2 level, the EOM space includes the one-hole-one-particle (1h1p) and the two-hole-two-particle (2h2p) configurations, while the three-hole-three-particle (3h3p) and four-hole-four-particle (4h4p) configurations are further added at the CC3 and CC4 levels, respectively. These two schemes produce identical IPs and satellite energies but, for a given level of theory, the diagonalization in the N -electron sector is more computationally demanding due to the larger size of the EOM space (see Ref. 296 for more details). In each scheme, the desired states have been obtained thanks to the root-following Davidson algorithm implemented in CFOUR. The initial vectors were built using the dominant configurations of the SCI vectors.

The Δ CCSD(T) calculations have been performed with GAUSSIAN16.²⁶³ These calculations are based on a closed-shell restricted HF reference and an open-shell unrestricted HF reference for the neutral and cationic species, respectively.¹⁴⁹

C. Green’s function calculations

Many-body Green’s function calculations have been carried out with the open-source software QUACK.²⁹⁷ In the following, we use the acronyms G_0W_0 , $G_0F(2)$, and G_0T_0 to refer to the one-shot schemes where one relies on the GW , second-Born, and T -matrix self-energies, respectively. Each approximated scheme considered in this work (G_0W_0 , $qsGW$, $G_0F(2)$, and G_0T_0) relies on HF quantities as starting point. We refer the reader to Refs. 81 and 150 for additional details about the theory and implementation of these methods. The infinitesimal broadening parameter η is set to $0.001 E_h$ for all calculations. It is worth mentioning that we do not linearize the quasiparticle equation to obtain the quasiparticle energies. The $qsGW$ calculations are performed with the regularized scheme based on the similarity renormalization group approach, as described in Ref. 113. A flow parameter of $s = 500$ is employed. All (occupied and virtual) orbitals are corrected. The spectral weight of each quasiparticle solution is reported in Supporting Information. Compared to the EOM-CC formalism discussed in Sec. II B, it is important to mention that, in the Green’s function framework, the IP and EA sectors [*i.e.* the 1h and one-particle (1p) configurations] are actually coupled,^{150,281,298} effectively creating higher-order diagrams.^{82,298}

III. RESULTS AND DISCUSSION

The present section is partitioned into subsections, each dedicated to a distinct group of related molecules. Within these subsections, we focus our attention mainly on the satellite states while IPs are addressed in Sec. III G.

Each state considered in this work is reported alongside its symmetry label, *e.g.* 1^2B_1 for the principal IP of water. Furthermore, the main orbitals involved in the ionization process are specified. For example, the N -electron ground state of water has the following dominant configuration $(1a_1)^2(2a_1)^2(1b_2)^2(3a_1)^2(1b_1)^2$, while the configuration of the $(N - 1)$ -electron ground state is $(1a_1)^2(2a_1)^2(1b_2)^2(3a_1)^2(1b_1)^1$. Hence, we denote the principal IP as $(1b_1)^{-1}$ to indicate that an electron has been ionized from the $1b_1$ orbital. The lowest satellite of water, *i.e.* the 2^2B_1 state of configuration $(1a_1)^2(2a_1)^2(1b_2)^2(3a_1)^1(1b_1)^1(4a_1)^1$, is labeled as $(3a_1)^{-1}(1b_1)^{-1}(4a_1)^1$ to signify that one electron was detached from the orbital $1b_1$ and $3a_1$, one of them being subsequently promoted to the virtual orbital $4a_1$ and the other ionized. In some cases, additional valence complete-active-space CI calculations have been performed using MOLPRO to determine the symmetry of the FCI states.²⁹⁹

A. 10-electron molecules: Ne, HF, H₂O, NH₃, and CH₄

The water molecule has been extensively studied experimentally using photoionization and electron impact

TABLE I. Valence ionizations and satellite transition energies (in eV) of the 10-electron series for various methods and basis sets. AVXZ stands for aug-cc-pVXZ (where X = D, T, and Q). Selected experimental values are also reported.

Methods	Basis				Basis				Basis			
	6-31+G*	AVDZ	AVTZ	AVQZ	6-31+G*	AVDZ	AVTZ	AVQZ	6-31+G*	AVDZ	AVTZ	AVQZ
Mol.	Water (H ₂ O)				Water (H ₂ O)				Water (H ₂ O)			
State/Conf.	$1^2B_1/(1b_1)^{-1}$				$1^2A_1/(3a_1)^{-1}$				$1^2B_2/(1b_2)^{-1}$			
Exp.	12.6 ²⁰⁴				14.8 ²⁰⁴				18.7 ²⁰⁴			
CC2	11.159	11.345	11.541	11.620	13.513	13.645	13.791	13.863	18.035	18.039	18.145	18.211
CCSD	12.170	12.386	12.594	12.675	14.502	14.677	14.825	14.895	18.861	18.888	18.972	19.032
CC3	12.287	12.519	12.661	12.722	14.621	14.811	14.899	14.949	18.950	18.993	19.023	19.065
CCSDT	12.276	12.491	12.629	12.689	14.601	14.776	14.861	14.910	18.919	18.951	18.981	19.022
CC4	12.307	12.543	12.683	12.741	14.635	14.832	14.920	14.968	18.952	18.999	19.030	19.070
CCSDTQ	12.304	12.534	12.673	×	14.631	14.822	14.907	×	18.947	18.990	19.018	×
FCI	12.309	12.540	12.679	12.737	14.636	14.829	14.915	14.962	18.950	18.995	19.024	19.063
G ₀ W ₀	12.312	12.485	12.884	13.080	14.625	14.781	15.106	15.285	18.818	18.865	19.129	19.290
qsGW	12.379	12.640	12.879	12.982	14.696	14.932	15.107	15.197	18.965	19.069	19.188	19.271
G ₀ F(2)	11.110	11.279	11.555	11.675	13.507	13.626	13.837	13.945	17.983	17.978	18.141	18.236
G ₀ T ₀	11.967	12.095	12.357	×	14.240	14.336	14.532	×	18.459	18.429	18.572	×
Mol.	Ammonia (NH ₃)				Ammonia (NH ₃)				Ammonia (NH ₃)			
State/Conf.	$1^2A_1/(3a_1)^{-1}$				$1^2E/(1e_g)^{-1}$				$3^2A_1/(2a_1)^{-1}$			
Exp.	10.93 ³⁰⁰				16.6 ³⁰⁰							
CC2	9.779	9.986	10.168	10.234	15.794	15.828	15.960	16.019	27.646	27.381	27.365	×
CCSD	10.434	10.677	10.862	10.923	16.403	16.473	16.588	16.639	27.745	27.696	27.855	27.915
CC3	10.447	10.746	10.888	10.935	16.407	16.520	16.592	16.629	27.252	27.114	27.191	×
CCSDT	10.449	10.734	10.876	10.922	16.399	16.500	16.573	16.609	26.773	26.724	26.899	×
CC4	10.461	10.761	10.901	×	16.417	16.533	16.603	×	26.669	26.621	26.746	×
CCSDTQ	10.461	10.760	10.899	×	16.415	16.529	16.598	×	26.698	26.645	26.768	×
FCI	10.463	10.762	10.901	10.945	16.418	16.534	16.603	16.640	26.683	26.659	26.779	26.833(1)
G ₀ W ₀	10.675	10.837	11.201	11.362	16.527	16.578	16.867	17.007	28.241	28.117	28.427	28.463
qsGW	10.520	10.870	11.094	11.176	16.468	16.655	16.805	16.878	28.029	27.962	27.980	28.151
G ₀ F(2)	9.841	9.994	10.244	10.345	15.817	15.814	16.002	16.088	27.589	27.638	27.729	×
G ₀ T ₀	10.399	10.497	10.716	×	16.217	16.170	16.330	×	28.860	28.738	28.860	×
Mol.	Methane (CH ₄)				Methane (CH ₄)				Methane (CH ₄)			
State/Conf.	$1^2T_2/(1t_2)^{-1}$				$1^2A_1/(2a_1)^{-1}$				$1^2\Pi/(1\pi)^{-1}$			
Exp.	14.5 ³⁰¹				23.0 ³⁰¹				16.19 ³⁰²			
CC2	13.787	13.888	14.028	14.079	23.289	23.227	23.311	23.352	14.431	14.559	14.725	14.813
CCSD	14.102	14.258	14.387	14.428	23.238	23.247	23.383	23.426	15.688	15.837	16.021	16.117
CC3	14.060	14.270	14.365	14.395	23.034	23.035	23.138	23.173	15.917	16.036	16.126	16.194
CCSDT	14.068	14.269	14.365	14.395	23.040	23.035	23.135	23.171	15.885	15.992	16.077	16.145
CC4	14.072	14.284	14.376	×	23.039	23.050	23.142	×	15.947	16.068	16.161	16.227
CCSDTQ	14.073	14.284	14.376	×	23.042	23.052	23.143	×	15.935	16.051	16.140	16.205
FCI	14.073	14.285	14.377	14.407	23.043	23.056	23.146	23.148(10)	15.941	16.059	16.149	16.214
G ₀ W ₀	14.338	14.466	14.753	14.872	23.647	23.626	23.875	23.988	15.679	15.868	16.237	16.453
qsGW	14.142	14.446	14.621	14.686	23.248	23.426	23.550	23.605	16.001	16.144	16.349	16.469
G ₀ F(2)	13.861	13.913	14.102	14.176	23.377	23.257	23.385	23.447	14.280	14.437	14.685	14.815
G ₀ T ₀	14.117	14.117	14.275	×	24.107	24.051	24.163	×	15.334	15.466	15.721	×
Mol.	Hydrogen fluoride (HF)				Neon (Ne)				Neon (Ne)			
State/Conf.	$1^2\Sigma^+/(3\sigma)^{-1}$				$1^2P/(2p)^{-1}$				$1^2S/(2s)^{-1}$			
Exp.	19.90 ³⁰²				21.57 ³⁰³				48.46 ³⁰³			
CC2	18.740	18.814	18.908	18.982	19.874	20.017	20.144	20.236	47.483	47.265	47.187	47.207
CCSD	19.777	19.861	19.946	20.021	21.030	21.168	21.326	21.432	48.735	48.363	48.426	48.494
CC3	19.980	20.040	20.050	20.100	21.353	21.417	21.449	21.522	48.652	48.263	48.145	48.168
CCSDT	19.933	19.989	19.995	20.045	21.304	21.367	21.398	21.473	48.725	48.330	48.229	48.270
CC4	19.986	20.051	20.065	20.114	21.375	21.434	21.473	21.546	48.829	48.424	48.316	48.349
CCSDTQ	19.974	20.036	20.046	20.094	21.362	21.421	21.455	21.527	48.811	48.406	48.293	48.326
FCI	19.979	20.043	20.054	20.102	21.365	21.426	21.461	21.533	48.822	48.417	48.306	48.340
G ₀ W ₀	19.662	19.812	20.074	20.259	20.859	21.104	21.432	21.655	47.851	47.785	47.950	48.085
qsGW	19.984	20.084	20.203	20.304	21.361	21.435	21.592	21.729	47.844	47.652	47.560	47.566
G ₀ F(2)	18.644	18.744	18.899	19.007	19.642	19.851	20.066	20.202	47.246	47.082	47.055	47.096
G ₀ T ₀	19.312	19.402	19.551	×	20.671	20.847	21.085	×	48.966	48.851	48.886	×
Mol.	Water (H ₂ O)				Water (H ₂ O)				Water (H ₂ O)			
State/Conf.	$2^2B_1/(3a_1)^{-1}(1b_1)^{-1}(4a_1)^1$				$2^2A_1/(1b_1)^{-2}(4a_1)^1$				$3^2B_1/(3a_1)^{-1}(1b_1)^{-1}(4a_1)^1$			
Exp.	27.1 ²⁰⁴				27.1 ²⁰⁴							
CC3	26.152	25.797	26.075	26.174	25.949	25.763	26.038	26.130	27.654	27.425	27.661	27.747
CCSDT	27.566	27.694	28.103	28.246	27.324	27.476	27.831	27.954	29.005	29.129	29.442	29.559
CC4	26.894	26.844	27.090	27.195	26.943	26.965	27.159	27.239	28.588	28.580	28.737	28.813
CCSDTQ	27.051	27.049	27.297	×	27.065	27.104	27.294	×	28.714	28.729	28.882	×
FCI	27.062	27.065	27.300	27.389	27.084	27.131	27.312	27.404	28.731	28.754	28.899	28.973
Mol.	Ammonia (NH ₃)				Ammonia (NH ₃)				Ammonia (NH ₃)			
State/Conf.	$2^2A_1/(3a_1)^{-2}(4a_1)^1$				$2^2E/(3a_1)^{-2}(3e)^1$				$2^2T_2/(1t_2)^{-2}(3a_1)^1$			
Exp.									29.2 ³⁰¹			
CC3	23.112	23.126	23.367	23.440	25.489	25.220	25.418	25.471	28.102	28.188	28.388	28.445
CCSDT	23.866	24.101	24.408	24.503	25.881	25.882	26.113	26.189	28.210	28.415	28.643	28.713
CC4	23.579	23.764	23.952	×	25.666	25.618	25.743	×	27.922	28.111	28.271	×
CCSDTQ	23.631	23.818	24.003	×	25.688	25.648	25.773	×	27.931	28.123	28.282	×
FCI	23.630	23.829	24.004	24.061	25.685	25.655	25.771	25.815	27.859	28.108	28.238	28.277(5)
Mol.	Hydrogen fluoride (HF)				Hydrogen fluoride (HF)				Hydrogen fluoride (HF)			
State/Conf.	$2^2\Sigma^+/(1\pi)^{-2}(4\sigma)^1$				$1^2\Delta/(1\pi)^{-2}(4\sigma)^1$							
Exp.												
CC3	31.076	30.636	30.916	×	32.872	32.516	32.749	32.852				
CCSDT	32.849	32.917	33.356	33.531	34.845	34.885	35.218	35.365				
CC4	32.110	31.981	32.210	×	34.309	34.181	34.304	34.399				
CCSDTQ	32.312	32.228	32.466	32.603	34.503	34.403	34.528	34.631				
FCI	32.347	32.257	32.474	32.605	34.547	34.445	34.554	34.648				

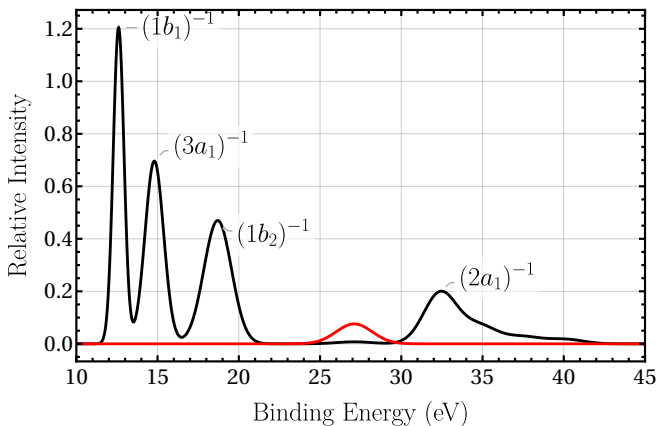


FIG. 1. Gaussian fit of the experimental ionization spectrum of water in gas phase measured by Ning and coworkers. The fitting parameters can be found in Ref. 204. The red peak at 27.1 eV has been magnified by a factor 10.

spectroscopy.^{204,304,305} For example, a high-resolution spectrum of liquid water is crucial as a first step for understanding the photoelectron spectra of aqueous phases.^{5,6} On the other hand, its gas-phase ionization spectrum is now well understood. The experimental ionization spectrum of water is plotted in Fig. 1, serving as a representative example to illustrate the following discussion. The first three sharp peaks at 12.6, 14.8, and 18.7 eV are associated with electron detachments from the three outer-valence orbitals, $1b_1$, $3a_1$, and $1b_2$, respectively.²⁰⁴ Then, a broader yet intense peak corresponding to the fourth ionization, $(2a_1)^{-1}$, is found at 32.4 eV surrounded by several close-lying satellite peaks. Additionally, there is a smaller broad satellite peak at 27.1 eV (magnified red peak in Fig. 1).

Table I gathers the FCI reference values corresponding to the three lowest satellites identified in our study. The first two, which are of 2B_1 and 2A_1 symmetries, lie close to each other around 27.1 eV. The third satellite is of 2B_1 symmetry and is found at slightly higher energy, approximately 29 eV. The ordering and the absolute energies of the three satellites align well with previous SAC-CI results reported by Ning *et al.*²⁰⁴ In addition, they showed that, at the ADC(3) level, the energy of the $2\ {}^2A_1$ state is overestimated by approximately 2.7 eV while the $2\ {}^2B_1$ and $3\ {}^2B_1$ states are missing. It is also worth noting that early CI and Green’s function studies had qualitatively predicted the $2\ {}^2A_1$ satellite.^{12,187} Finally, we do not consider the broad peak at 32.4 eV here because it is technically out of reach for our current SCI implementation. However, it has been studied by Mejuto-Zaera and coworkers who have shown that vertex corrections are required to correctly describe this complex part of the spectrum where strong many-body effects are at play.¹³

For the three satellites of water, CCSDTQ is in near-perfect agreement with FCI in all basis sets with errors inferior to 0.03 eV. CC4 is slightly worse than CCSDTQ but is still an excellent approximation given its lower

computational cost and its approximate treatment of quadruples. The CCSDT satellite energies are overestimated by approximately 0.5 eV, while CC3 appears to struggle for this system. Indeed, the CC3 energies are badly underestimated with errors up to 1.5 eV, and the ordering of the first two satellites is wrongly predicted.³⁰⁶ Finally, CCSD and CC2 are not considered for satellites as their poor performance (wrong by several eV) makes the assignment of these states extremely challenging.

The remainder of this section is concerned with four molecules isoelectronic to water, namely CH_4 , NH_3 , HF, and Ne. For each of these molecules, Table I provides FCI reference values for the IPs corresponding to the two outermost valence orbitals. In addition, two satellite energies are reported for hydrogen fluoride and ammonia while one satellite is presented for methane. Experimental values for the IPs of these four molecules have been measured multiple times and are reported in Table I.^{4,7,189,191,192,300,302,307–309}

Yencha and coworkers measured the inner-valence photoelectron spectrum of HF. It displays a well-defined peak around 33 eV which appears in close agreement with the FCI energies for the $2\ {}^2\Sigma^+$ state.³⁰⁹ In addition, a doubly-degenerate satellite of ${}^2\Delta$ symmetry has also been computed. In the various NH_3 ionization spectra reported in the literature, there is no satellite peak around 24 eV which may correspond to the $2\ {}^2A_1$ and $2\ {}^2E$ FCI states.^{189,201,300} Nevertheless, the FCI energies align well with the SAC-CI energies of Ishida and coworkers who predicted that these two satellite states have very low intensity.²⁰¹ The first satellite observed in the inner-valence region of the photoionization spectrum of CH_4 is a very weak and broad peak at 29.2 eV.³⁰¹ This peak is also measured at 28.56 eV using electron momentum spectroscopy experiments.¹⁹² The energy of the first satellite calculated at the FCI level, and associated with the $(2t_2)^{-2}(3a_1)^1$ process, compares well with the experimental data. It is worth noting that CC3 behaves similarly in HF and H_2O , yet it appears to be a much better approximation for the satellite states of NH_3 and CH_4 .

Among the 12 IPs computed for this series of molecules, 11 of them have a weight larger than 0.85 on the 1h dominant configuration (in the aug-cc-pVDZ basis set). Only the $3\ {}^2A_1$ state of ammonia has a quite smaller weight (0.58) on the corresponding 1h determinant. This exemplifies the breakdown of the orbital picture in the inner-valence ionization spectrum,^{12,169–181} which signature is a significant weight on both 1h and 2h1p configurations, hence preventing us from assigning the solution as a clear IP or satellite. The performance of the various approximations for IPs will be statistically gauged in Sec. III G.

TABLE II. Satellite transition energies of ammonia and water computed with Green’s function methods in the aug-cc-pVDZ basis set. The FCI values are reported for comparison purposes.

Molecule	State	Method	Diag. element	Eigenvalue	FCI
NH ₃	2 ² A ₁	G ₀ F(2)	24.324	24.328	23.829
		G ₀ W ₀	24.408	24.410	
		G ₀ T ₀	40.441	40.444	
NH ₃	2 ² E	G ₀ F(2)	24.977	24.977	25.655
		G ₀ W ₀	24.997	24.997	
		G ₀ T ₀	41.094	41.094	
H ₂ O	2 ² B ₁	G ₀ F(2)	30.759	30.759	27.065
		G ₀ W ₀	30.846	30.846	
		G ₀ T ₀	×	×	
H ₂ O	2 ² A ₁	G ₀ F(2)	28.683	28.683	27.131
		G ₀ W ₀	28.770	28.770	
		G ₀ T ₀	×	×	
H ₂ O	3 ² B ₁	G ₀ F(2)	30.759	30.781	28.754
		G ₀ W ₀	30.863	30.867	
		G ₀ T ₀	×	×	

B. Satellite in Green’s functions methods

Thus far, we have exclusively assessed the performance of different rungs of the CC hierarchy. Although shake-up transition energies can also be computed within the Green’s function framework, the task is notably more challenging, especially when compared to the more straightforward nature of IP-EOM-CC. This complexity arises from the fact that satellites, existing as non-linear solutions of the quasiparticle equation,⁷⁹ prove much more difficult to converge using Newton-Raphson algorithms than the quasiparticle solutions, which are representative of typical IPs. Fortunately, an alternative and equivalent pathway exists where one solves a larger linear eigenvalue problem instead of solving the non-linear quasiparticle equation.^{82,125,150,282,310–314} In such a case, satellites are obtained as higher-energy roots via diagonalization of the so-called “upfolded” matrix built in the basis of the 2h1p and two-particle-one-hole (2p1h) configurations in addition to the 1h and 1p configurations.

The satellite energies of H₂O and NH₃ computed with G₀W₀, G₀F(2), and G₀T₀ are presented in Table II. qsGW is not considered here as its static approximation naturally discards all the satellite solutions. The third column shows the diagonal elements of the upfolded matrix associated with the 2h1p configurations, while the fourth column displays the associated eigenvalues. One can immediately observe that the eigenvalues do not improve upon the diagonal elements. This is due to the lack of higher-order (such as 3h2p) configurations that are essential to correlate satellites. This parallels the description of double excitations which require at least triple excitations (*i.e.* 3h3p configurations) in addition to the 2h2p configurations to correlate doubly-excited states.^{9–11} Regarding the two satellites of ammonia, the *T*-matrix zeroth-order elements are utterly inaccurate. This discrepancy arises because,

at the *T*-matrix level, satellite energies are described as the sum of a Koopmans’ electron attachment energy (1p configuration) and a double electron detachment energy [two-hole (2h) configuration] stemming from the particle-particle random-phase approximation.^{150,315–318} On the other hand, G₀W₀ and G₀F(2) offer decent estimates of these satellite energies.

The remaining three rows of Table II contain the energies corresponding to the three satellites of water discussed previously. The 2 ²A₁ state is the easiest to identify as its 2h1p dominant configuration clearly corresponds to the (1b₁)⁻²(4a₁)¹ process. The eigenvectors associated with the 2 ²B₁ and 3 ²B₁ states, which correspond to the (3a₁)⁻¹(1b₁)⁻¹(4a₁)¹ and (1b₁)⁻¹(3a₁)⁻¹(4a₁)¹ processes respectively, are nearly degenerate and highly entangled. This is thus harder, if not impossible, to assign these states.

Because of these assignment problems, the G₀W₀, G₀F(2), and G₀T₀ satellite energies have not been computed for the other molecules considered in this study. To alleviate this issue, there is a notable appeal for a self-energy approximation including vertex corrections capable of effectively addressing satellite states. As mentioned previously, Green’s-function-based methods such as the 2ph-TDA¹⁷¹ and ADC(3)^{180,319,320} (first named extended 2ph-TDA¹⁷⁹) have shown success in qualitatively modeling the inner-valence region of experimental spectra.^{12,169–179,181,321} Sokolov’s recent multi-reference ADC(2) scheme³²² is also a promising avenue. In particular, it has shown potential in describing the satellites of the carbon dimer (see below).^{234,235} While a detailed quantitative analysis of these approaches on the present benchmark set would be interesting, it lies beyond the scope of this study.

C. 14-electron molecules: N₂, CO, and BF

The nitrogen and carbon monoxide molecules have been extensively studied both experimentally^{324–330} and theoretically.^{39,169,180,182,183,185,197,331–333} Their ionization spectra are similar as they exhibit three sharp and intense peaks, corresponding to Koopmans’ states, below 20 eV. Their respective fourth IP, corresponding to electron detachment from the orbital 2σ_g for N₂ and 3σ for CO, lies above 30 eV. Several peaks can be found below these ionizations, *i.e.* between 20 and 30 eV.^{324,327,328} These correspond to satellite states associated with the three outer-valence orbitals. Note that Schirmer *et al.* have shown (using the 2ph-TDA method¹⁷¹) that the quasiparticle approximation breaks down in the region of the fourth ionizations of CO and N₂.^{169,180} However, as shown below, the peaks between 20 and 30 eV have a well-defined satellite character.

Baltzer *et al.* produced, using He(II) photoelectron spectroscopy, accurate experimental values for the outer-valence IPs (see Table III) and the first satellite peaks of N₂.³²⁵ In particular, they reported a value of 25.514 eV

TABLE III. Valence ionizations and satellite transition energies (in eV) of the 14-electron series for various methods and basis sets. AVXZ stands for aug-cc-pVXZ (where X = D, T, and Q). Selected experimental values are also reported.

Methods	Basis				Basis				Basis			
	6-31+G*	AVDZ	AVTZ	AVQZ	6-31+G*	AVDZ	AVTZ	AVQZ	6-31+G*	AVDZ	AVTZ	AVQZ
Mol.					Boron fluoride (BF)							
State/Conf.	$1^2\Sigma^+/(5\sigma)^{-1}$				$2^2\Pi/(1\pi)^{-1}$				$2^2\Sigma^+/(4\sigma)^{-1}$			
Exp.	11.06 ³²³											
CC2	10.751	10.824	10.944	10.987	17.136	17.274	17.385	17.467	19.767	19.957	19.962	20.041
CCSD	11.080	11.154	11.250	11.279	17.920	18.028	18.172	18.246	21.017	21.208	21.253	21.342
CC3	10.914	11.004	11.100	11.127	18.606	18.722	18.743	18.794	20.745	20.910	20.918	20.984
CCSDT	10.969	11.057	11.157	11.185	18.474	18.584	18.622	18.677	20.708	20.866	20.875	20.946
CC4	10.965	11.053	11.148	11.175	18.475	18.593	18.626	18.679	20.770	20.920	20.917	20.981
CCSDTQ	10.967	11.054	11.150	×	18.453	18.569	18.599	×	20.734	20.882	20.874	×
FCI	10.966	11.054	11.149	11.175	18.466	18.581	18.612	18.664	20.765	20.913	20.906	20.970(1)
G_0W_0	11.053	11.117	11.325	11.420	18.237	18.456	18.743	18.949	21.142	21.402	21.567	21.778
qsGW	10.862	10.989	11.167	11.240	18.513	18.662	18.784	18.899	21.389	21.583	21.585	21.701
$G_0F(2)$	10.859	10.915	11.052	11.114	16.958	17.132	17.328	17.454	19.654	19.878	19.955	20.079
G_0T_0	10.821	10.856	10.955	×	17.947	18.105	18.304	×	20.739	20.955	21.041	×
Mol.					Carbon monoxide (CO)							
State/Conf.	$1^2\Sigma^+/(5\sigma)^{-1}$				$1^2\Pi/(1\pi)^{-1}$				$2^2\Sigma^+/(4\sigma)^{-1}$			
Exp.	14.01 ³²⁴				17.0 ³²⁴				19.7 ³²⁴			
CC2	13.550	13.584	13.748	13.809	16.289	16.349	16.505	16.581	18.175	18.316	18.400	18.464
CCSD	13.948	13.998	14.190	14.246	16.793	16.865	17.024	17.095	19.501	19.657	19.790	19.867
CC3	13.614	13.697	13.863	13.912	16.826	16.902	17.018	17.075	19.512	19.664	19.744	19.807
CCSDT	13.693	13.770	13.952	14.005	16.762	16.838	16.960	17.016	19.347	19.498	19.583	19.647
CC4	13.678	13.760	13.933	13.984	16.751	16.835	16.955	17.009	19.410	19.566	19.653	19.715
CCSDTQ	13.679	13.761	13.935	×	16.755	16.837	16.958	×	19.376	19.532	19.616	×
FCI	13.670	13.752	13.925	13.975	16.762	16.845	16.966	17.017(2)	19.393	19.550	19.637	19.699(1)
G_0W_0	14.461	14.467	14.777	14.915	16.677	16.762	17.083	17.264	19.869	20.045	20.300	20.485
qsGW	13.980	14.080	14.318	14.416	16.836	16.932	17.124	17.231	19.899	20.071	20.191	20.298
$G_0F(2)$	13.856	13.857	14.067	14.154	16.134	16.204	16.422	16.534	18.165	18.317	18.460	18.564
G_0T_0	14.163	14.143	14.324	×	16.422	16.470	16.666	×	19.333	19.481	19.613	×
Mol.					Dinitrogen (N ₂)							
State/Conf.	$1^2\Sigma_g^+/(3\sigma_g)^{-1}$				$1^2\Pi_u/(1\pi_u)^{-1}$				$1^2\Sigma_u^+/(2\sigma_u)^{-1}$			
Exp.	15.580 ³²⁵				16.926 ³²⁵				18.751 ³²⁵			
CC2	14.613	14.649	14.814	14.877	16.932	16.943	17.104	17.178	17.803	17.862	17.991	18.037
CCSD	15.382	15.424	15.641	15.709	17.065	17.087	17.228	17.287	18.654	18.721	18.931	18.991
CC3	15.282	15.349	15.519	15.574	16.669	16.719	16.837	16.885	18.598	18.680	18.849	18.899
CCSDT	15.270	15.333	15.517	15.574	16.765	16.812	16.950	17.001	18.502	18.585	18.763	18.816
CC4	15.220	15.293	15.471	15.526	16.770	16.821	16.940	16.987	18.403	18.493	18.669	18.720
CCSDTQ	15.237	15.309	15.487	×	16.764	16.815	16.936	×	18.429	18.519	18.696	×
FCI	15.235	15.308	15.486	15.541	16.759	16.811	16.933	16.981	18.427	18.516	18.692	18.742
G_0W_0	15.959	15.984	16.350	16.519	16.781	16.790	17.093	17.259	19.515	19.558	19.862	20.000
qsGW	15.575	15.663	15.914	16.020	16.640	16.706	16.903	17.006	19.125	19.221	19.425	19.513
$G_0F(2)$	14.824	14.845	15.080	15.181	16.956	16.952	17.158	17.261	17.974	18.020	18.201	18.274
G_0T_0	15.494	15.502	15.722	×	16.673	16.653	16.820	×	18.993	19.021	19.190	×
Mol.					Boron Fluoride (BF)							
State/Conf.	$1^2\Pi/(5\sigma)^{-2}(2\pi)^1$											
Exp.												
CC3	17.494	17.541	17.607	17.637								
CCSDT	17.410	17.462	17.532	17.567								
CC4	17.293	17.345	17.393	17.419								
CCSDTQ	17.303	17.355	17.405	×								
FCI	17.297	17.346	17.392	17.417								
Mol.					Carbon monoxide (CO)							
State/Conf.	$2^2\Pi/(5\sigma)^{-2}(2\pi)^1$				$2^2\Sigma^+/(1\pi)^{-1}(5\sigma)^{-1}(2\pi)^1$				$1^2\Delta/(1\pi)^{-1}(5\sigma)^{-1}(2\pi)^1$			
Exp.	22.7 ³²⁴				23.7 ³²⁴							
CC3	23.406	23.507	23.597	23.640	23.640	23.729	23.839	23.881	23.730	23.814	23.926	23.968
CCSDT	23.205	23.313	23.441	23.507	23.381	23.472	23.602	23.669	23.417	23.503	23.647	23.713
CC4	22.862	22.957	22.997	23.040	23.102	23.166	23.193	23.236	23.143	23.206	23.251	23.293x
CCSDTQ	22.841	22.937	22.995	×	23.101	23.167	23.209	×	23.141	23.205	23.264	×
FCI	22.791	22.889	22.908(1)	22.962(3)	23.074(1)	23.140(2)	23.194(1)	23.232(1)	23.114	23.181	23.233	23.271(1)
Mol.					Dinitrogen (N ₂)							
State/Conf.	$1^2\Pi_g/(3\sigma_g)^{-2}(4\pi_g)^1$				$1^2\Sigma_u^+/(3\sigma_g)^{-1}(3\pi_u)^{-1}(4\pi_g)^1$				$1^2\Sigma_u^-/(3\sigma_g)^{-1}(3\pi_u)^{-1}(4\pi_g)^1$			
Exp.	24.788 ³²⁵				25.514 ³²⁵							
CC3	25.280	25.331	25.495	25.535	25.656	25.699	25.856	25.908	26.584	26.599	26.686	26.723
CCSDT	24.945	25.008	25.232	25.304	25.405	25.453	25.643	25.721	26.209	26.250	26.362	26.427
CC4	24.394	24.458	24.575	24.621	25.099	25.142	25.235	25.288	25.990	26.012	26.022	26.058
CCSDTQ	24.363	24.431	24.574	×	25.088	25.134	25.238	×	25.721	25.756	25.762	×
FCI	24.277	24.348	24.470(1)	24.519(1)	25.054	25.103	25.199	×	25.658	25.695	25.689	×

for an intense satellite peak, as well as 24.788 eV for a very weak peak. These peaks were assigned $2^2\Sigma_u^+$ and $2^2\Pi_g$ symmetry, respectively, based on CI calculations. Note that the $2^2\Pi_g$ satellite peak is more intense when measured

by resonance Auger spectroscopy.³²⁴ We report FCI values for both satellites as well as a slightly higher third one with $2^2\Sigma_u^-$ symmetry. This latter state is not observed experimentally but plays an important role nonetheless

as it is involved in the dissociation pathways between the $2^2\Sigma_u^+$ and $4^1\Pi_u$ states.³³¹

Similar to its isoelectronic N_2 molecule, CO exhibits shake-up peaks between the $(4\sigma)^{-1}$ and $(3\sigma)^{-1}$ ionizations. Using monochromatized X-ray excited photoelectron spectroscopy, Svensson *et al.* observed an intense $2^2\Sigma^+$ satellite peak with energy 23.7 eV as well as a weak $2^2\Pi$ satellite at 22.7 eV.³²⁴ This is in agreement with older He(II) photoelectron spectroscopy experiments done by Asbrink and coworkers.³²⁸ FCI values for both satellites, as well as for the higher-energy $1^2\Delta$ state, are reported in Table II.

The performance of CC schemes for these six satellites is similar to what we have observed for the 10-electron series. Yet, it is interesting to note that CCSDTQ seems to struggle slightly more with the $2^2\Pi$ satellite of CO and the $1^2\Pi_g$ and $1^2\Sigma_u^-$ states of N_2 .

The boron fluoride molecule is isoelectronic to CO and N_2 but its ionization spectrum is much harder to obtain experimentally because BF is a quite non-volatile compound, meaning that the measurements have to be done at high temperatures.³²³ Yet, Hildenbrand and coworkers managed to measure its principal IP using electron impact spectroscopic and they reported a value of 11.06 eV. The $1^2\Sigma^+$ FCI state is in good agreement with this value. Table II also displays two additional IPs and one satellite. The order of the $2^2\Pi$ states in BF is reversed with respect to its isoelectronic species: the $(5\sigma)^{-2}(2\pi)^1$ satellite state has a lower energy than the $(1\pi)^{-1}$ ionization. In this case, CCSDTQ accurately describes the satellite of Π symmetry.

D. 12-electron molecules: LiF, BeO, BN, and C_2

We now direct our attention toward the 12-electron isoelectronic molecules: LiF, BeO, BN, and C_2 . These four molecules are quite challenging for theoretical methods as, except for LiF, their ground states have a strong multi-reference character.^{335–342} For example, BN and BeO are among the eight molecules of the GW100 set having multiple solution issues at the GW level.^{24,25} (C_2 is not considered in the GW100 set but would certainly fall in the same category.) Another noteworthy observation about these molecules is that their lowest unoccupied molecular orbital has a negative energy, which means that their respective anions are stable.

LiF is a relatively non-volatile molecule, and as a result, experimental data became accessible during the second phase of the development of ultraviolet photoelectron spectroscopy.³³⁴ In addition, lithium fluoride vapor is not solely composed of monomers but also includes dimers, trimers, or even tetramers, posing challenges for more precise measurements of the Koopmans states of LiF. Berkowitz *et al.* measured the first two IPs using He(I) photoelectron spectroscopy: 11.50, 11.67, and 11.94 eV for the $1^2\Pi_{3/2,3/2}$, $1^2\Pi_{3/2,1/2}$, and $1^2\Sigma^+$ states, respectively. In our study, the spin-orbit coupling is not accounted for.

Therefore, we report a single value for the $1^2\Pi$ state, while experimentally two distinct ionization energies are measured.

To the best of our knowledge, no gas phase experimental values are available for the three remaining species (see Ref. 343 for a study in solid phase). Nonetheless, they are an interesting playground for theoretical methods due to their multi-reference character. We start by discussing BeO as it has the less pronounced multi-reference character out of these three molecules. Table IV displays the excitation energies of the two lowest Koopmans states and the first two satellites. These four states have the same dominant configurations and ordering as the ones of lithium fluoride. However, the satellite states of BeO are much lower in energy than those of LiF. The $2^2\Pi$ state of BeO is interesting as it exhibits the largest error of this benchmark set at the CCSDTQ level. At the CC4 level, the $2^2\Pi$ and $1^2\Sigma^-$ states are drastically underestimated. This is also the case for the two satellite states of LiF, these four states having, by far, the largest CC4 errors of this benchmark set. They are also hugely underestimated at the CC3 level and, as for CC2 and CCSD, we have not reported these energies as they are not meaningful. Unfortunately, at this stage, we have no clear explanation for the failure of CC3 and CC4 in LiF and BeO.

BN and C_2 have the strongest multi-reference character among these four molecules.³⁴² The ordering of their state differs from the one of LiF and BeO as their lowest satellite states are below their second IP. Furthermore, the ordering of the satellites is also different than the two previous molecules. The first satellite of boron nitride has the same dominant configuration as in the latter two molecules but the second satellite is of $1^2\Delta$ symmetry with a $(1\pi)^{-2}(5\sigma)^1$ dominant process. This satellite is also found in C_2 but even lower in the energy spectrum as the $1^2\Delta_g$ state is the lowest-energy satellite of the carbon dimer. Table IV reports two additional FCI satellite transition energies of C_2 . Note that the satellite transition energies of BeO, BN, and C_2 are the lowest of the present set. The three satellite states of the carbon dimer have already been studied by Chatterjee and Sokolov.^{234,235} In particular, they have shown that ADC(3) performs poorly and does not even predict enough satellite states. On the other hand, their extension of ADC(2) using a multi-determinantal reference³²² can predict each state and be in quantitative agreement with FCI.^{234,235}

E. Third-row molecules: CS, Ar, HCl, H_2S , PH_3 , SiH_4 , and LiCl

The molecules examined in this subsection have been obtained by substituting a second-row atom with its third-row analog in some of the molecules discussed above. These molecules with more diffuse density have their ionization shifted towards zero with respect to their second-row counterparts (see Tables V, VI, and VII). Consequently, the breakdown of the orbital picture occurs at

TABLE IV. Valence ionizations and satellite transition energies (in eV) of the 12-electron series for various methods and basis sets. AVXZ stands for aug-cc-pVXZ (where X = D, T, and Q). Selected experimental values are also reported.

Methods	Basis				Basis				Basis			
	6-31+G*	AVDZ	AVTZ	AVQZ	6-31+G*	AVDZ	AVTZ	AVQZ	6-31+G*	AVDZ	AVTZ	AVQZ
Mol.	Lithium fluoride (LiF)				Beryllium oxide (BeO)							
State/Conf.	$1^2\Pi/(1\pi)^{-1}$				$1^2\Sigma^+/(4\sigma)^{-1}$				$1^2\Pi/(1\pi)^{-1}$			
Exp.	11.50,11.67 ³³⁴				11.94 ³³⁴							
CC2	9.481	9.588	9.804	9.895	9.801	9.923	10.109	10.209	9.615	9.712	9.818	9.894
CCSD	11.078	11.193	11.398	11.493	11.566	11.701	11.874	11.979	9.708	9.808	9.875	9.941
CC3	11.142	11.222	11.375	11.449	11.588	11.682	11.802	11.883	9.976	10.096	10.243	10.320
CCSDT	11.165	11.247	11.379	11.452	11.641	11.738	11.834	11.914	9.750	9.849	9.864	9.916
CC4	11.270	11.351	11.496	11.567	11.764	11.863	11.971	12.049	9.749	9.850	9.867	9.922
CCSDTQ	11.234	11.315	11.453	×	11.719	11.816	11.917	×	9.831	9.930	9.939	×
FCI	11.246	11.328	11.468	11.538	11.735	11.833	11.933	12.018(2)	9.863	9.962	9.972	10.018
G_0W_0	10.797	10.979	11.384	11.594	11.339	11.549	11.915	12.139	9.356	9.489	9.727	9.907
qsGW	11.249	11.330	11.575	11.699	11.809	11.926	12.119	12.255	9.991	10.079	10.168	10.251
$G_0F(2)$	9.294	9.445	9.729	9.857	9.644	9.812	10.063	10.200	7.957	8.072	8.195	8.302
G_0T_0	10.512	10.644	10.923	×	10.968	11.120	11.366	×	8.885	8.975	9.108	×
Mol.	Beryllium oxide (BeO)				Boron nitride (BN)							
State/Conf.	$1^2\Sigma^+/(4\sigma)^{-1}$				$1^2\Pi/(1\pi)^{-1}$				$1^2\Sigma^+/(4\sigma)^{-1}$			
Exp.												
CC2	10.523	10.620	10.667	10.735	10.734	10.792	10.927	10.991	12.842	12.870	12.979	13.018
CCSD	10.861	10.987	11.006	11.082	11.776	11.850	11.971	12.018	13.571	13.624	13.697	13.720
CC3	11.128	11.269	11.370	11.454	11.825	11.941	12.057	12.101	13.641	13.718	13.806	13.828
CCSDT	10.830	10.962	10.916	10.975	11.778	11.871	11.980	12.019	13.642	13.716	13.790	13.808
CC4	10.825	10.959	10.915	10.977	11.681	11.797	11.902	11.940	13.534	13.626	13.700	13.718
CCSDTQ	10.923	11.056	11.007	×	11.754	11.860	11.966	×	13.580	13.667	13.745	×
FCI	10.970	11.103	11.056	11.115(2)	11.767	11.875	11.980	12.019	13.571	13.660	13.729(11)	13.710(70)
G_0W_0	10.628	10.798	10.996	11.200	11.423	11.447	11.752	11.907	13.154	13.171	13.447	13.590
qsGW	11.083	11.199	11.241	11.341	11.597	11.711	11.898	11.987	13.376	13.490	13.621	13.693
$G_0F(2)$	8.499	8.648	8.720	8.837	10.817	10.857	11.031	11.122	12.207	12.195	12.382	12.454
G_0T_0	9.930	10.064	10.155	×	10.988	10.996	11.159	×	12.499	12.512	12.657	×
Mol.	Carbon dimer (C_2)											
State/Conf.	$1^2\Pi_u/(2\pi_u)^{-1}$											
Exp.												
CC2	12.742	12.779	12.951	13.023								
CCSD	12.770	12.830	12.978	13.030								
CC3	11.930	12.058	12.177	12.215								
CCSDT	12.289	12.391	12.540	12.585								
CC4	12.231	12.347	12.472	12.511								
CCSDTQ	12.225	12.340	12.471	×								
FCI	12.205	12.323	12.463	12.497								
G_0W_0	12.621	12.613	12.928	13.082								
qsGW	12.202	12.344	12.561	12.656								
$G_0F(2)$	12.882	12.870	13.078	13.175								
G_0T_0	12.482	12.454	12.625	×								
Mol.	Carbon dimer (C_2)											
State/Conf.	$1^2\Delta_g/(2\pi_u)^{-2}(3\sigma_g)^1$				$1^2\Sigma_g^+/(2\pi_u)^{-2}(3\sigma_g)^1$				$1^2\Sigma_g^+/(2\pi_u)^{-2}(3\sigma_g)^1$			
Exp.												
CC3	14.644	14.713	14.815	14.850	14.846	14.957	15.087	15.123	15.360	15.353	15.435	15.460
CCSDT	14.494	14.568	14.680	14.729	14.721	14.833	14.998	15.051	15.086	15.072	15.194	15.246
CC4	13.920	14.007	14.052	14.076	14.196	14.308	14.359	14.388	14.304	14.331	14.413	14.439
CCSDTQ	13.879	13.969	14.041	×	14.182	14.200	14.310	×	14.209	14.316	14.423	×
FCI	13.798	13.889	13.944	13.963	14.084	14.099	14.167	14.193	14.108	14.244	14.337	14.359(1)
Mol.	Lithium fluoride (LiF)				Beryllium oxide (BeO)							
State/Conf.	$1^2\Sigma^-/(1\pi)^{-2}(5\sigma)^1$				$2^2\Pi/(4\sigma)^{-1}(1\pi)^{-1}(5\sigma)^1$				$1^2\Sigma^-/(1\pi)^{-2}(5\sigma)^1$			
Exp.												
CC3	×	×	×	×	×	×	×	×	×	×	×	×
CCSDT	26.917	27.177	27.738	27.945	27.545	27.810	28.345	28.559	15.515	15.699	16.062	16.206
CC4	24.868	25.062	25.341	×	25.125	25.295	25.565	×	13.215	13.376	×	×
CCSDTQ	25.937	26.105	26.401	×	26.464	26.632	26.900	×	14.198	14.349	14.517	×
FCI	25.958	26.118	26.381	×	26.471	26.627	26.856	27.016(1)	14.095	14.244	14.380	×
Mol.	Beryllium oxide (BeO)				Boron nitride (BN)							
State/Conf.	$2^2\Pi/(4\sigma)^{-1}(1\pi)^{-1}(5\sigma)^1$				$1^2\Sigma^-/(1\pi)^{-2}(5\sigma)^1$				$1^2\Delta/(1\pi)^{-2}(5\sigma)^1$			
Exp.												
CC3	×	×	×	×	13.120	13.132	13.270	13.289	13.299	13.331	13.489	13.517
CCSDT	17.306	17.501	17.826	17.984	13.432	13.515	13.795	13.870	13.942	14.024	14.252	14.315
CC4	13.361	13.558	×	×	12.569	12.627	12.758	12.790	13.221	13.289	13.383	13.402
CCSDTQ	15.677	15.840	15.954	×	12.510	12.582	12.739	×	13.244	13.324	13.431	×
FCI	15.455	15.616	15.683	15.805	12.393	12.463	12.600	×	13.185	13.263	13.351	13.357(21)

lower energy,¹⁷² which has been of interest historically as it allowed measuring spectra featuring such intricate structures more easily.

The first molecule considered in this subsection is carbon sulfide. In 1972, two independent studies measured

its photoelectron spectrum up to 20 eV.^{346,347} One can clearly distinguish four well-defined peaks in this energy range. While the assignment of the two lowest peaks is straightforward, *i.e.* IPs associated with the two outermost orbitals, the interpretation of the other two remained

TABLE V. Valence ionizations and satellite transition energies (in eV) of the third-row molecules for various methods and basis sets. AVXZ stands for aug-cc-pVXZ (where X = D, T, and Q). Selected experimental values are also reported.

Methods	Basis				Basis				Basis			
	6-31+G*	AVDZ	AVTZ	AVQZ	6-31+G*	AVDZ	AVTZ	AVQZ	6-31+G*	AVDZ	AVTZ	AVQZ
Mol.	Carbon sulfide (CS)								$2^2\Sigma^+/(6\sigma)^{-1}$			
State/Conf.	$1^2\Sigma^+/(7\sigma)^{-1}$				$1^2\Pi/(2\pi)^{-1}$							
Exp.												
CC2	10.627	10.745	10.847	10.900	12.791	12.897	13.014	13.083	16.698	16.817	16.945	17.005
CCSD	11.245	11.402	11.553	11.609	12.726	12.883	13.000	13.059	16.854	16.997	17.220	17.288
CC3	10.949	11.186	11.325	11.377	12.553	12.766	12.880	12.937	18.201	18.290	18.389	18.422
CCSDT	10.966	11.190	11.346	11.404	12.596	12.799	12.918	12.974	17.915	18.023	18.134	18.179
CC4	10.914	11.161	11.310	11.368	12.542	12.764	12.878	12.934	17.764	17.881	17.959	17.994
CCSDTQ	10.920	11.166	11.316	×	12.548	12.768	12.885	×	17.749	17.865	17.947	×
FCI	10.899	11.151	11.300	11.355	12.545	12.768	12.882(1)	12.936	17.723	17.844	17.920	17.958(2)
G_0W_0	12.092	12.119	12.378	12.523	12.602	12.679	12.907	13.063	17.666	17.713	17.976	18.119
qsGW	11.369	11.589	11.775	11.880	12.498	12.705	12.852	12.958	17.323	17.505	17.688	17.788
$G_0F(2)$	11.109	11.152	11.292	11.371	12.696	12.774	12.923	13.018	16.704	16.779	16.942	17.026
G_0T_0	11.595	11.594	11.713	×	12.479	12.505	12.609	×	17.422	17.455	17.591	×
Mol.	Carbon sulfide (CS)								$1^2\Delta/(2\pi)^{-1}(7\sigma)^{-1}(3\pi)^1$			
State/Conf.	$2^2\Sigma^+/(2\pi)^{-1}(7\sigma)^{-1}(3\pi)^1$				$3^2\Sigma^+/(2\pi)^{-1}(7\sigma)^{-1}(3\pi)^1$							
Exp.												
CC3	16.183	16.329	16.500	16.560	17.358	17.491	17.558	17.584	17.448	17.558	17.635	17.662
CCSDT	15.921	16.089	16.278	16.352	16.986	17.145	17.208	17.264	17.039	17.178	17.266	17.319
CC4	15.677	15.863	15.997	16.059	16.628	16.799	16.773	16.807	16.701	16.861	16.871	16.902
CCSDTQ	15.646	15.838	15.982	×	16.600	16.772	16.754	×	16.678	16.840	16.858	×
FCI	15.604	15.803	15.935	15.996(1)	16.551	16.727	16.691	16.728(2)	16.632	16.800	16.802	16.837(2)
Mol.	Lithium chloride (LiCl)								$1^2\Sigma^+/(6\sigma)^{-1}$			
State/Conf.	$1^2\Pi/(2\pi)^{-1}$				$1^2\Sigma^+/(6\sigma)^{-1}$							
Exp.	9.98,10.06 ³⁴⁴				10.77 ³⁴⁴							
CC2	9.215	9.396	9.535	9.639	9.902	10.109	10.189	10.299				
CCSD	9.604	9.830	9.956	10.067	10.327	10.566	10.637	10.757				
CC3	9.529	9.788	9.880	9.992	10.235	10.518	10.552	10.671				
CCSDT	9.533	9.787	9.883	9.993	10.241	10.517	10.554	10.673				
CC4	9.556	9.811	9.898	×	10.265	10.544	10.573	×				
CCSDTQ	9.552	9.808	9.896	×	10.261	10.540	10.570	×				
FCI	9.555	9.810	9.897	10.007	10.267	10.545	10.577	10.696				
G_0W_0	9.611	9.734	9.984	10.180	10.357	10.500	10.690	10.897				
qsGW	9.574	9.808	9.947	10.086	10.307	10.569	10.642	10.789				
$G_0F(2)$	9.222	9.365	9.551	9.676	9.916	10.083	10.210	10.341				
G_0T_0	9.567	9.619	9.761	×	10.274	10.360	10.448	×				
Mol.	Lithium chloride (LiCl)								Fluorine (F ₂)			
State/Conf.	$2^2\Sigma^+/(2\pi)^{-2}(7\sigma)^1$				$2^2\Pi/(6\sigma)^{-1}(2\pi)^{-1}(7\sigma)^1$				$2^2\Sigma_g^+/(1\pi_u)^{-1}(1\pi_g)^{-1}(3\sigma_u)^1$			
Exp.												
CC3	18.447	18.788	19.156	19.328	19.055	19.402	19.717	19.897	22.465	22.584	22.866	22.934
CCSDT	19.582	20.043	20.508	20.729	20.304	20.745	21.168	21.397	22.293	22.387	22.663	22.758
CC4	18.837	19.326	19.639	×	19.477	19.959	20.224	×	22.050	22.064	22.177	22.234
CCSDTQ	18.963	19.468	19.788	×	19.645	20.141	20.413	×	22.025	22.038	22.174	×
FCI	18.942	19.446	19.741	19.955	19.617	20.115	20.357	20.577	22.024(2)	22.039(1)	22.165(1)	22.224(4)
Mol.	Fluorine (F ₂)								$1^2\Sigma_g^+/(3\sigma_g)^{-1}$			
State/Conf.	$1^2\Pi_g/(1\pi_g)^{-1}$				$1^2\Pi_u/(1\pi_u)^{-1}$				$1^2\Sigma_g^+/(3\sigma_g)^{-1}$			
Exp.	15.8 ³⁴⁵				18.9 ³⁴⁵				20.9 ³⁴⁵			
CC2	13.903	14.001	14.145	14.233	17.050	17.122	17.224	17.297	20.325	20.458	20.522	20.604
CCSD	15.279	15.405	15.616	15.722	18.633	18.753	18.946	19.047	21.068	21.155	21.174	21.241
CC3	15.574	15.646	15.746	15.825	18.786	18.847	18.924	18.994	21.091	21.155	21.130	21.182
CCSDT	15.529	15.594	15.688	15.767	18.745	18.797	18.865	18.936	21.048	21.109	21.094	21.148
CC4	15.555	15.621	15.701	15.804	18.746	18.797	18.864	18.941	21.086	21.142	21.146	21.171
CCSDTQ	15.559	15.623	15.725	×	18.754	18.803	18.874	×	21.077	21.132	21.106	×
FCI	15.564	15.628	15.729	15.808	18.758	18.807	18.874	18.943(1)	21.077	21.132	21.100(2)	21.149
G_0W_0	15.763	15.964	16.334	16.559	19.423	19.589	19.902	20.104	20.434	20.625	20.836	21.029
qsGW	15.927	16.016	16.229	16.368	19.524	19.585	19.752	19.875	20.855	20.934	21.000	21.114
$G_0F(2)$	13.809	13.960	14.194	14.328	16.965	17.087	17.275	17.389	20.137	20.308	20.420	20.534
G_0T_0	15.026	15.157	15.401	×	18.615	18.724	18.928	×	19.934	20.083	20.190	×

elusive for several years. Thanks to theoretical studies performed several years later, it became clear that the third peak is due to a multi-particle process while the fourth one is associated with an electron detachment from the orbital 6σ .^{172,234,235,306} Note that, as explained by Schirmer *et al.*,¹⁷² one has to be particularly careful when labeling the third peak as a satellite because its FCI vector has a coefficient of 0.49 on the $1h$ configuration $(6\sigma)^{-1}$ and of 0.40 on the $2h1p$ configuration $(2\pi)^{-1}(7\sigma)^{-1}(3\pi)^1$ (in 6-31+G* basis set). This is yet another example of a

strong configuration mixing.

Despite this, the $2^2\Sigma^+$ state is classified as a satellite in Table V. Indeed, higher in energy there is another FCI solution of $2^2\Sigma^+$ symmetry with an even larger weight, 0.63, on the $1h$ determinant $(6\sigma)^{-1}$ and coefficients smaller than 0.31 on the $2h1p$ determinants. In addition, the third peak has a pronounced vibrational structure while the fourth peak is sharp like the $(7\sigma)^{-1}$ one.³⁴⁷ This is why the higher $2^2\Sigma^+$ state is classified as the third single ionization in Table V. Two other satellite states,

$3\ ^2\Sigma^+$ and $1\ ^2\Delta$, that are not visible on the experimental spectrum, are reported in Table V.

Next, we consider lithium chloride and compare it with its second-row analog, lithium fluoride. The experimental challenges outlined earlier for LiF are similar for LiCl. Experimental values have first been reported independently by two groups in 1979,^{334,348} and revised values, measured by He(I) spectroscopy, have been published recently,³⁴⁴ and are reported in Table V. The FCI results predict two close-lying satellites around 20 eV. Unfortunately, the experimental studies mentioned above do not probe this energy range. The ADC(3) calculations of Tomasello *et al.* also predict two satellite lines around 21.5 eV.³⁴⁹

Finally, we examine the 18-electron isoelectronic hydrides as analogs to the 10-electron series discussed in Subsec. III A. Historically, it was quickly realized that the satellite structure of H₂S is significantly more complex than the one of H₂O.¹⁷⁴ This intricate structure can be observed in the electron momentum spectrum of French *et al.*³⁵⁰ They recorded a first very weak satellite at 19.63 eV which is in agreement with earlier measurements³⁵¹ as well as photoelectron spectrum measured using synchrotron radiation.³⁵² Several years later, extensive SAC-CI results have been reported and show qualitative agreement with experiments.²⁰⁰ (See also earlier calculations from Refs. 193 and 195.) However, the FCI results (see Table VII) exhibit some significant difference with the SAC-CI results of Ehara *et al.* because the $2\ ^2A_1$ satellite has a lower energy than the $2\ ^2B_2$ state. In addition, the FCI transition energy associated with the $2\ ^2B_1$ state is 2 eV lower than the one computed in Ref. 200. The $2\ ^2A_1$ state is known to be the one observed at 19.63 eV in Ref. 350 and is sometimes referred to as a shake-down state as it “borrows” intensity from the higher-lying $(4a_1)^{-1}$ ionization.^{200,352,353} Our FCI estimate for this state is 18.745 eV while the SAC-CI energy of Ehara and collaborators is 20.00 eV.²⁰⁰ In this specific scenario, calculating the adiabatic transition energy related to this state would undoubtedly provide a more faithful comparison with the experimental result.

For PH₃, there is one satellite of symmetry E that is analog to the two $2\ ^2E$ state of NH₃. However, in the case of phosphine, there is no analog for the $2\ ^2A_1$ satellite of ammonia. This is in agreement with the SAC-CI results of Ishida *et al.* who also found a single satellite below the $(4a_1)^{-1}$ ionization threshold.²⁰¹

Two FCI states, with symmetry $2\Sigma^+$ and 2Δ , are reported for HCl. These states are analog to the HF satellites reported in Table I although they have significantly lower energies in HCl. The satellite structure between 20 eV and the $(4\sigma)^{-1}$ ionization around 26 eV is notably intricate.³⁵⁴ Additionally, this structure is characterized by weak signals and some of its features were even not observed in previous studies performed at a lower level of theory.^{355–357} The assignment of the various peaks in this energy range is beyond the scope of this work. Yet, one can mention that the first FCI satellite is in qualitative agreement with the first satellite peak measured by

synchrotron radiation spectroscopy at 21.57 eV.³⁵⁴

F. Miscellaneous molecules: F₂, CO₂, CH₂O, and BH₃

In this last subset, a few miscellaneous molecules are considered. First, the F₂ molecule is of interest as it is isoelectronic to SiH₄, PH₃, H₂S, HCl and Ar. Due to the absence of third-row atoms in F₂, Cederbaum *et al.* observed that there is no breakdown of the orbital picture, as observed in the 18-electron hydride series.¹⁷⁰ Three IPs and one satellite transition energy of fluorine are reported in Table V. As documented in Ref. 170, these four states have a clear dominant configuration in their corresponding FCI vectors. The $2\ ^2\Sigma_g^+$ satellite is not observed in photoionization^{302,358} or in electron impact spectra.³⁴⁵ However, a satellite state with the same symmetry and similar energy has been computed using ADC(4) and multi-reference CI.³⁴⁵

Carbon dioxide and formaldehyde are two small organic molecules that have been widely studied both experimentally and theoretically. Experimental studies have shown that CO₂ first measurable satellite peak is around 22 eV,^{188,205,326,359} while four ionization peaks are observed below 20 eV. Tian’s experimental values for these IPs, measured by electron momentum spectroscopy, are reported alongside our FCI estimates in Table VIII.²⁰⁵ These IPs have already been computed at various levels of theory such as CI,¹⁸⁸ ADC,^{234,235,359} SAC-CI,^{194,205} CC,³⁵ and even FCI.^{234,235}

The spectrum of formaldehyde is slightly harder to interpret. The electron momentum spectrum displays a sharp peak at 10.9 eV as well as a broad band between 12 and 18 eV.¹⁹⁰ On the other hand, one can observe four different peaks below 17 eV in the corresponding photoionization spectra.^{177,360} These peaks clearly correspond to ionizations from the four outermost orbitals (see Table VIII) and have already been computed using both wave function and Green’s function methods.^{35,38,177,234,235,332} Hochlaf *et al.* also mention a very weak band around 18 eV assigned as a satellite of $2B_2$ symmetry,³⁶⁰ which can also be observed in Ref. 177. This is in nice agreement with the $3\ ^2B_2$ FCI satellite state. There is an additional $2\ ^2B_1$ satellite state with slightly lower energy than the previous one.

Finally, a small boron hydride is considered as we have seen above that boron-containing molecules such as BN are quite challenging. To the best of our knowledge, experimental results on BH₃ are quite scarce but the principal IP has been measured using mass spectroscopy in the 60’s.^{361,362} These two research groups reported quite different values of 12.32 eV³⁶¹ and 11.4 eV.³⁶² The FCI values, presented in Table VIII, is closer to the first one, corroborating the findings of Tian *et al.*, who computed similar values using propagator-based methods as well as CCSD(T).³⁶³ Finally, two FCI satellite transition energies of BH₃ are reported in Table VIII.

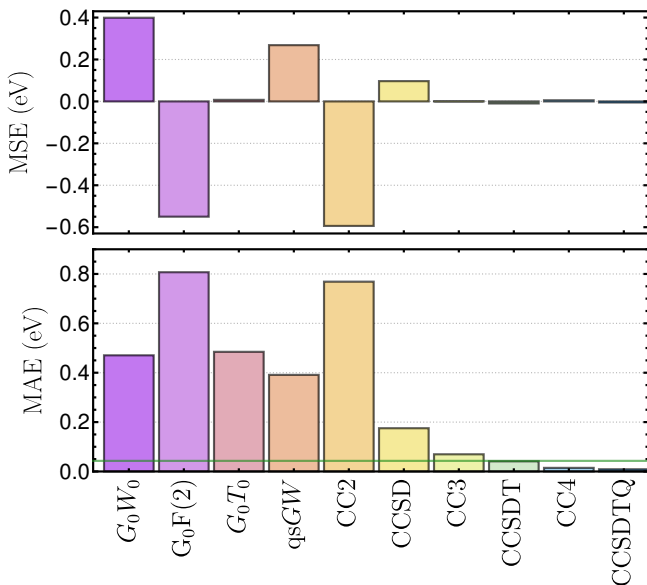


FIG. 2. Mean signed error (MSE) [upper panel] and mean absolute error (MAE) [lower panel] with respect to FCI of the various methods considered in this work. These errors are computed for the 58 IPs of this set in the aug-cc-pVTZ basis set.

TABLE VI. Mean absolute error (MAE), mean signed error (MSE), root mean square error (RMSE), standard deviation error (SDE), minimum and maximum errors (in eV) with respect to FCI of the various methods considered in this work. These descriptors are computed for the 58 IPs of this set in the aug-cc-pVTZ basis set. The Δ CCSD(T) statistical descriptors correspond only to the 23 principal IPs.

Methods	MAE	MSE	RMSE	SDE	Min	Max
CC2	0.769	-0.594	0.940	0.735	-2.207	1.565
CCSD	0.175	0.097	0.280	0.265	-0.700	1.075
CC3	0.070	0.001	0.125	0.126	-0.395	0.469
CCSDT	0.041	-0.010	0.057	0.057	-0.140	0.214
CC4	0.015	0.005	0.027	0.027	-0.078	0.118
CCSDTQ	0.010	-0.005	0.013	0.012	-0.049	0.027
G_0W_0	0.470	0.399	0.664	0.535	-0.504	2.053
qsGW	0.391	0.268	0.559	0.494	-1.348	1.747
$G_0F(2)$	0.807	-0.550	0.987	0.827	-2.336	1.623
G_0T_0	0.485	0.007	0.752	0.758	-1.169	2.959
Δ CCSD(T)	0.021	0.016	0.037	0.035	-0.020	0.120

G. Global statistics

Finally, after discussing each molecule individually, the statistics over the whole set are reported and discussed in this subsection. Figure 2 displays the mean sign error (MSE) and MAE of the various methods considered in this study with respect to the new FCI references. These statistical errors have been computed for the 58 IPs in the aug-cc-pVTZ basis set. Several other statistical descriptors are also reported in Table VI.

The CC hierarchy (CCSD, CCSDT, and CCSDTQ)

behaves as expected, *i.e.* being more and more accurate as the rank of the excitation is increased. Chemical accuracy (*i.e.*, error below 0.043 eV as represented by the horizontal green line in the lower panel Fig. 2) is reached at the CCSDT level. The least expensive CC2 method does not perform well for IPs as already observed previously.^{364–366} This has been attributed to the same underlying issue observed in CC2 for Rydberg³⁶⁷ and charge-transfer excited states.³⁶⁸

Figure 2 also shows that CC3 and CC4 are good approximations, for IPs, of their respective parents, CCSDT and CCSDTQ. This could have been expected for CC3 as it is known to be a good approximation of CCSDT for Rydberg excited states.³⁶⁷ In addition, these four methods have very small MSEs and do not, on average, underestimate (as CC2) or overestimate (as CCSD) the IPs. Therefore, implementations of IP-EOM-CC3 and IP-EOM-CC4 would be valuable to lower the cost of the present implementation based on EE-EOM. CC3 and CC4 could be certainly employed as reference methods for larger molecular systems.^{240,290,369}

For the sake of completeness, we also report in Table VI the statistical descriptors for the propagator methods. However, their trends are now well-known.^{113,142,149,150} The G_0T_0 MAE is very close to the G_0W_0 one whereas the second-Born approximation exhibits significantly poorer performance.^{142,149,150} The self-consistent qsGW slightly mitigates the error compared to the one-shot *GW* version. It is also interesting to note that GF2 results are very close to those of CC2. This could have been expected as GF2 is equivalent to ADC(2)^{82,124,150} and the latter is closely related to the CC2 approximation.³⁷⁰

Finally, the principal IP of the 23 molecules considered so far have been computed at the Δ CCSD(T) in the aug-cc-pVTZ basis set (see [Supporting Information](#)). This method has been used as the reference for the *GW*100 dataset and it is interesting to benchmark it now that we have access to FCI references.^{25,61,149,371} The last line of Table VI reports the corresponding statistical descriptor. In particular, its MAE and MSE of 0.021 eV and 0.016 eV, respectively, show that the state-specific Δ CCSD(T) method can indeed be employed as a reference.

Figure 3 shows the distribution of the errors associated with the satellite transitions computed with CC methods including at least triple excitations, namely, CC3, CCSDT, CC4, and CCSDTQ. The corresponding statistical descriptors are reported in Table VII. The MAE of CCSDTQ is 0.040 eV, *i.e.* just below chemical accuracy, while CC4 and its approximate treatment of quadruples achieve a 0.087 eV MAE. Interestingly, while CC4 absolute errors are, on average, larger than CCSDTQ, its MSE is closer to zero. CC3 and CCSDT have MAEs of 0.749 eV and 0.528 eV, respectively, and once again CC3 and CC4 have lower MSEs than their parent methods (0.232 eV and 0.528 eV). Hence, methods accounting for triple excitations, even fully, should be used with care for satellites. It is also interesting to note that these

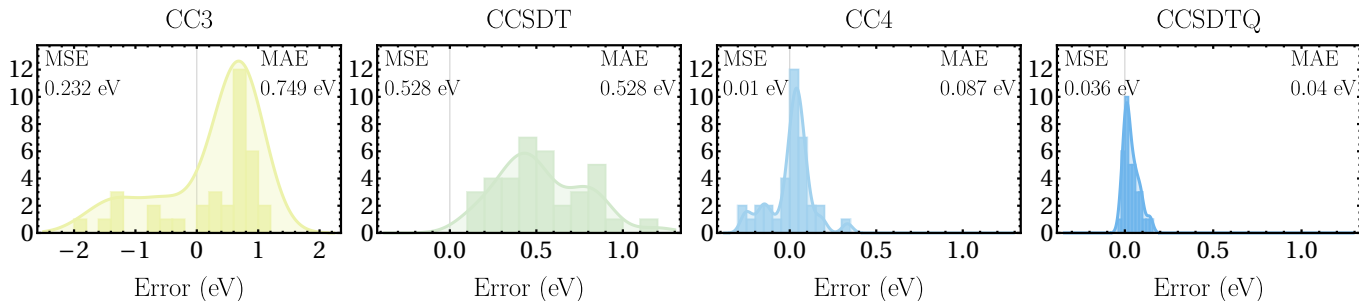


FIG. 3. Distribution of the errors with respect to FCI of the various methods considered in this work. These errors are computed for the 36 satellites of this set in the aug-cc-pVTZ basis set. The satellites of LiF and BeO have been excluded (see main text). Note the different scale of the horizontal axis in the leftmost plot.

TABLE VII. Mean absolute error (MAE), mean signed error (MSE), root mean square error (RMSE), standard deviation error (SDE), minimum and maximum errors (in eV) with respect to FCI of the various methods considered in this work. These descriptors are computed for the 36 satellites of this set in the aug-cc-pVTZ basis set. The satellites of LiF and BeO have been excluded (see main text).

Methods	MAE	MSE	RMSE	SDE	Min	Max
CC3	0.749	0.232	0.830	0.809	-1.805	1.098
CCSDT	0.528	0.528	0.582	0.249	0.104	1.195
CC4	0.087	0.010	0.118	0.119	-0.264	0.333
CCSDTQ	0.040	0.036	0.055	0.043	-0.026	0.143

MAEs align very well with those computed for double excitations, as reported in Ref. 10.

IV. CONCLUSION

We have reported 40 FCI satellite transition energies computed in 23 small molecules. These energies have been calculated with increasingly large basis sets ranging from Pople’s 6-31+G* to Dunning’s aug-cc-pVXZ (where X = D, T, and Q). In addition, 58 FCI reference values for outer- and inner-valence IPs of the same molecular set have been presented. This work is the tenth layer of reference values of the QUEST database^{23,238} and the first one to include charged excitations.

Various CC methods have been employed to compute IPs (CC2, CCSD, CC3, CCSDT, CC4, and CCSDTQ) and satellite transition energies (CC3, CCSDT, CC4, and CCSDTQ), and their performances have been assessed using the FCI reference values. It has been shown that CC3 and CC4 are faithful approximations of CCSDT and CCSDTQ for IPs, respectively, while the CC2 approximate treatment of double excitations induces large errors with respect to CCSD. For the satellites, our study reveals that chemical accuracy is reached only at the CCSDTQ level, highlighting the intricate and complex correlation effects involved in such states and their overall challenging nature for computational methods.

The performance of various propagator methods (G_0W_0 , $G_0F(2)$, G_0T_0 , and qsGW) have also been gauged. The poor performance of these methods for satellite transition energies has been discussed in detail. These results call for the development of new methods capable of describing such states. Studying the convergence of the ADC hierarchy using these new benchmark values is a possible outlook. Finally, assessing methods designed in the condensed matter community, such as the cumulant Green’s function, on these small molecular systems would certainly be interesting. Work along this line is presently underway.

One obvious perspective that needs to be addressed is the extension to transition intensities, which are of crucial importance for direct comparisons with experimental spectra. An approximate electronic structure method should not only aim to accurately describe the excited-state energy but also the transition intensities associated with it. Within the present SCI formalism, computing intensities is not straightforward but this is feasible, as demonstrated in Refs. 13, 373, and 374, and is planned for future investigation.

ACKNOWLEDGMENTS

This project has received funding from the European Research Council (ERC) under the European Union’s Horizon 2020 research and innovation programme (Grant agreement No. 863481). This work used the HPC resources from CALMIP (Toulouse) under allocations 2023-18005 and 2024-18005. The authors thank Abdallah Ammar, Fabris Kossoski, Yann Damour, Alexander Sokolov, Devin Matthews, Anthony Scemama, and Denis Jacquemin for helpful comments and/or insightful discussions.

SUPPORTING INFORMATION

The [Supporting Information](#) includes the geometry of the 23 molecules considered in this study as well as a json

TABLE VIII. Valence ionizations and satellite transition energies (in eV) of the 18-electron series for various methods and basis sets. AVXZ stands for aug-cc-pVXZ (where X = D, T, and Q). Selected experimental values are also reported.

Methods	Basis				Basis				Basis			
	6-31+G*	AVDZ	AVTZ	AVQZ	6-31+G*	AVDZ	AVTZ	AVQZ	6-31+G*	AVDZ	AVTZ	AVQZ
Mol.					(H ₂ S)							
State/Conf.	$1^2B_1/(2b_1)^{-1}$				$1^2A_1/(5a_1)^{-1}$				$1^2B_2/(2b_2)^{-1}$			
Exp.	10.5 ³⁵⁰				13.1 ³⁵⁰				15.6 ³⁵⁰			
CC2	9.699	9.953	10.156	10.228	12.833	13.004	13.155	13.220	15.393	15.368	15.464	15.521
CCSD	9.908	10.208	10.421	10.490	13.057	13.280	13.440	13.497	15.540	15.591	15.684	15.734
CC3	9.846	10.189	10.388	10.454	12.985	13.259	13.407	13.459	15.475	15.567	15.635	15.680
CCSDT	9.853	10.190	10.390	10.455	12.985	13.253	13.399	13.450	15.460	15.552	15.619	15.664
CC4	9.855	10.199	10.394	10.458	12.990	13.265	13.407	13.456	15.458	15.560	15.624	15.668
CCSDTQ	9.855	10.199	10.393	×	12.990	13.265	13.406	×	15.457	15.558	15.622	×
FCI	9.855	10.199	10.393	10.456	12.992	13.268	13.411	13.460	15.459	15.562	15.627	15.672
G ₀ W ₀	10.034	10.172	10.500	10.660	13.212	13.339	13.614	13.758	15.684	15.698	15.928	16.058
qsGW	9.890	10.201	10.445	10.549	13.048	13.337	13.530	13.619	15.524	15.651	15.785	15.868
G ₀ F(2)	9.747	9.940	10.180	10.282	12.887	13.005	13.188	13.278	15.420	15.364	15.494	15.569
G ₀ T ₀	9.927	10.011	10.188	×	13.068	13.112	13.250	×	15.588	15.477	15.582	×
Mol.					(PH ₃)							
State/Conf.	$1^2A_1/(5a_1)^{-1}$				$1^2E/(2e_g)^{-1}$				$2^2A_1/(4a_1)^{-1}$			
Exp.	10.85 ²⁰¹				16.4 ²⁰¹				27.6 ²⁰¹			
CC2	10.030	10.219	10.392	10.444	13.463	13.493	13.638	13.689	21.308	21.046	21.079	21.106
CCSD	10.198	10.448	10.623	10.662	13.521	13.637	13.784	13.825	20.144	20.221	20.361	20.396
CC3	10.130	10.431	10.599	10.634	13.464	13.615	13.744	13.779	19.528	19.643	19.739	19.763
CCSDT	10.129	10.431	10.599	10.634	13.454	13.606	13.734	13.769	19.317	19.487	19.583	19.610
CC4	10.127	10.436	10.600	×	13.452	13.611	13.737	×	19.263	19.446	19.520	×
CCSDTQ	10.127	10.437	10.600	×	13.451	13.611	13.737	×	19.259	19.442	19.511	×
FCI	10.126	10.436	10.596	10.628	13.456	13.615	13.745	13.784	19.261	19.445	19.514	19.537
G ₀ W ₀	10.365	10.497	10.787	10.911	13.717	13.831	14.099	14.214	21.505	21.378	21.567	21.673
qsGW	10.190	10.506	10.725	10.802	13.545	13.761	13.954	14.027	21.128	21.155	21.261	21.322
G ₀ F(2)	10.095	10.223	10.428	10.508	13.495	13.503	13.675	13.741	21.354	21.067	21.137	21.184
G ₀ T ₀	10.186	10.236	10.387	×	13.665	13.619	13.759	×	22.142	21.976	22.040	×
Mol.					(SiH ₄)							
State/Conf.	$1^2T_2/(2t_2)^{-1}$				$1^2A_1/(3a_1)^{-1}$				$1^2\Pi/(1\pi)^{-1}$			
Exp.	12.8 ³⁷²				18.2 ³⁷²				12.745/12.830 ³⁵⁴			
CC2	12.515	12.653	12.802	12.848	18.704	18.759	18.823	18.846	11.990	12.230	12.401	12.491
CCSD	12.477	12.701	12.844	12.877	18.266	18.379	18.483	18.505	12.250	12.538	12.712	12.812
CC3	12.417	12.681	12.806	12.832	18.109	18.236	18.316	18.331	12.186	12.529	12.672	12.771
CCSDT	12.407	12.673	12.794	12.820	18.046	18.172	18.247	18.262	12.190	12.524	12.667	12.764
CC4	12.404	12.676	12.795	×	18.033	18.171	18.241	×	12.199	12.539	12.678	12.773
CCSDTQ	12.404	12.677	12.795	×	18.030	18.170	18.238	×	12.199	12.538	12.676	×
FCI	12.403	12.676	12.793	12.818	18.031	18.173	18.240	18.258(2)	12.199	12.539	12.676	12.770
G ₀ W ₀	12.716	12.960	13.214	13.312	18.701	18.824	19.007	19.097	12.343	12.488	12.778	12.967
qsGW	12.541	12.906	13.107	13.170	18.422	18.700	18.828	18.879	12.224	12.539	12.723	12.855
G ₀ F(2)	12.550	12.662	12.830	12.886	18.742	18.768	18.855	18.899	12.022	12.200	12.415	12.535
G ₀ T ₀	12.712	12.762	12.891	×	19.119	19.156	19.204	×	12.273	12.347	12.507	×
Mol.					(HCl)							
State/Conf.	$1^2\Sigma^+/(5\sigma)^{-1}$				$1^2P/(3p)^{-1}$				$1^2S/(3s)^{-1}$			
Exp.	16.270 ³⁵⁴				15.8 ³⁰³				29.24 ³⁰³			
CC2	16.245	16.329	16.438	16.512	15.055	15.236	15.379	15.486	31.123	30.459	30.439	30.437
CCSD	16.467	16.599	16.708	16.782	15.308	15.534	15.672	15.802	30.353	29.838	29.881	29.907
CC3	16.395	16.577	16.658	16.730	15.230	15.525	15.614	15.745	30.255	29.437	29.238	29.227
CCSDT	16.388	16.564	16.644	16.715	15.228	15.514	15.606	15.735	30.261	29.445	29.214	29.216
CC4	16.394	16.577	16.653	16.723	15.238	15.531	15.616	15.743	30.263	29.442	29.186	29.179
CCSDTQ	16.393	16.576	16.651	×	15.237	15.529	15.614	15.740	30.261	29.442	29.182	29.175
FCI	16.396	16.579	16.657	16.728	15.237	15.529	15.613	15.739	30.265	29.449	29.188	29.182
G ₀ W ₀	16.574	16.635	16.872	17.031	15.333	15.458	15.711	15.926	31.226	30.759	31.089	31.224
qsGW	16.417	16.619	16.752	16.861	15.232	15.507	15.633	15.794	30.858	30.576	30.681	30.751
G ₀ F(2)	16.286	16.325	16.469	16.564	15.072	15.196	15.387	15.523	31.130	30.399	30.426	30.427
G ₀ T ₀	16.461	16.436	16.548	×	15.326	15.368	15.511	×	32.255	32.007	32.147	×
Mol.					Argon (Ar)							
State/Conf.	$2^2A_1/(2b_1)^{-2}(6a_1)^1$				$2^2B_2/(2b_1)^{-2}(3b_2)^1$				$2^2B_1/(5a_1)^{-1}(2b_1)^{-1}(6a_1)^1$			
Exp.	19.63 ³⁵⁰											
CC3	19.182	19.350	19.377	×	19.973	20.137	20.317	20.355	20.456	20.620	20.702	×
CCSDT	18.761	19.018	19.043	×	19.675	19.961	20.136	20.190	19.948	20.185	20.269	×
CC4	18.607	18.848	18.801	×	19.485	19.777	19.892	×	19.775	19.995	20.019	×
CCSDTQ	18.582	18.827	18.772	×	19.467	19.765	19.868	×	19.744	19.969	19.986	×
FCI	18.575	18.819	18.755	18.745	19.462	19.759	19.853	19.889	19.741	19.965	19.974	×
Mol.					(PH ₃)							
State/Conf.	2^2E				$2^2\Sigma^+/(2\pi)^{-1}(6\sigma)^1$				$1^2\Delta/(2\pi)^{-1}(6\sigma)^1$			
Exp.												
CC3	19.513	19.613	19.630	19.606	22.798	22.997	23.197	23.262	23.556	23.732	23.795	23.829
CCSDT	19.072	19.217	19.255	19.245	22.277	22.676	22.885	22.982	23.188	23.532	23.532	23.590
CC4	18.940	19.084	19.080	×	21.932	22.328	22.439	×	22.918	23.273	23.185	×
CCSDTQ	18.907	19.055	19.046	×	21.889	22.303	22.400	×	22.885	23.257	23.155	×
FCI	18.897	19.047	19.025	18.997	21.878	22.293	22.377	22.463	22.881	23.254	23.142	23.185

TABLE IX. Valence ionizations and satellite transition energies (in eV) of the remaining molecules for various methods and basis sets. AVXZ stands for aug-cc-pVXZ (where X = D, T, and Q). Selected experimental values are also reported.

Methods	Basis				Basis				Basis			
	6-31+G*	AVDZ	AVTZ	AVQZ	6-31+G*	AVDZ	AVTZ	AVQZ	6-31+G*	AVDZ	AVTZ	AVQZ
Mol.	Carbon dioxide (CO ₂)				Carbon dioxide (CO ₂)				Carbon dioxide (CO ₂)			
State/Conf.	$1^2\Pi_g/(1\pi_g)^{-1}$				$1^2\Pi_u/(1\pi_u)^{-1}$				$1^2\Sigma_u^+/(3\sigma_u)^{-1}$			
Exp.	13.8 ²⁰⁵				17.6 ²⁰⁵				18.1 ²⁰⁵			
CC2	12.747	12.812	13.015	13.103	16.508	16.630	16.751	16.829	16.866	16.889	17.034	17.107
CCSD	13.490	13.561	13.787	13.879	17.767	17.809	17.996	18.080	17.885	18.006	18.171	18.259
CC3	13.456	13.528	13.696	13.773	17.275	17.335	17.463	17.531	17.708	17.829	17.928	17.999
CCSDT	13.474	13.539	13.716	13.794	17.351	17.406	17.553	17.628	17.708	17.821	17.930	18.005
CC4	13.488	13.562	13.733	×	17.339	17.396	17.521	×	17.783	17.904	18.009	×
CCSDTQ	13.491	13.563	13.734	×	17.341	17.396	17.522	×	17.750	17.869	17.972	×
FCI	13.496	13.567	13.733	13.823	17.337	17.391	17.513(7)	17.618(6)	17.766(1)	17.889(1)	17.996(2)	×
G ₀ W ₀	13.743	13.837	14.221	14.425	18.184	18.209	18.519	18.697	18.335	18.474	18.791	18.994
qsGW	13.712	13.806	14.054	14.182	17.950	18.008	18.200	18.315	18.120	18.264	18.442	18.566
G ₀ F(2)	12.783	12.854	13.129	13.254	16.993	17.012	17.224	17.332	16.714	16.840	17.035	17.153
G ₀ T ₀	13.284	13.334	13.586	×	17.700	17.696	17.890	×	17.693	17.816	17.995	×
Mol.	Carbon dioxide (CO ₂)				Carbon dioxide (CO ₂)				Carbon dioxide (CO ₂)			
State/Conf.	$1^2\Sigma_g^+/(4\sigma_g)^{-1}$				$1^2\Sigma_g^+/(4\sigma_g)^{-1}$				$1^2\Sigma_g^+/(4\sigma_g)^{-1}$			
Exp.	19.4 ²⁰⁵				19.4 ²⁰⁵				19.4 ²⁰⁵			
CC2	17.746	17.864	17.980	18.048	×	×	×	×	×	×	×	×
CCSD	19.237	19.351	19.523	19.605	×	×	×	×	×	×	×	×
CC3	18.959	19.073	19.184	19.250	×	×	×	×	×	×	×	×
CCSDT	18.968	19.075	19.198	19.268	×	×	×	×	×	×	×	×
CC4	19.047	19.158	19.274	×	×	×	×	×	×	×	×	×
CCSDTQ	19.008	19.119	19.232	×	×	×	×	×	×	×	×	×
FCI	19.024(1)	19.137(2)	19.254(3)	×	×	×	×	×	×	×	×	×
G ₀ W ₀	19.730	19.856	20.150	20.334	×	×	×	×	×	×	×	×
qsGW	19.474	19.604	19.776	19.888	×	×	×	×	×	×	×	×
G ₀ F(2)	17.949	18.069	18.245	18.348	×	×	×	×	×	×	×	×
G ₀ T ₀	19.083	19.193	19.353	×	×	×	×	×	×	×	×	×
Mol.	Formaldehyde (CH ₂ O)				Formaldehyde (CH ₂ O)				Formaldehyde (CH ₂ O)			
State/Conf.	$1^2B_2/(2b_2)^{-1}$				$1^2B_1/(1b_1)^{-1}$				$1^2A_1/(5a_1)^{-1}$			
Exp.	10.9 ¹⁷⁷				14.5 ¹⁷⁷				16.1 ¹⁷⁷			
CC2	9.444	9.553	9.753	9.828	13.854	13.903	14.053	14.127	14.596	14.705	14.820	14.893
CCSD	10.486	10.625	10.848	10.924	14.410	14.480	14.606	14.667	15.833	15.964	16.105	16.181
CC3	10.555	10.710	10.873	10.932	14.377	14.482	14.562	14.609	15.832	15.985	16.063	16.119
CCSDT	10.533	10.680	10.840	10.898	14.381	14.478	14.562	14.609	15.811	15.953	16.030	16.086
CC4	10.578	10.736	10.897	×	14.395	14.504	14.578	×	15.879	16.039	16.114	×
CCSDTQ	10.574	10.729	10.887	×	14.391	14.498	14.572	×	15.864	16.018	16.090	×
FCI	10.582	10.739	10.899	10.954	14.395	14.502	14.578(1)	14.618(9)	15.876	16.032	16.106(1)	16.161(4)
G ₀ W ₀	10.835	10.996	11.380	11.556	14.232	14.283	14.587	14.759	16.170	16.292	16.602	16.794
qsGW	10.780	10.990	11.241	11.342	14.395	14.543	14.693	14.780	16.118	16.313	16.459	16.557
G ₀ F(2)	9.605	9.712	9.981	10.088	13.740	13.772	13.985	14.093	14.747	14.856	15.040	15.153
G ₀ T ₀	10.345	10.407	10.655	×	13.879	13.896	14.082	×	15.625	15.716	15.888	×
Mol.	Formaldehyde (CH ₂ O)				Borane (BH ₃)				Borane (BH ₃)			
State/Conf.	$2^2B_2/(1b_2)^{-1}$				$1^2E'/(1e')^{-1}$				$1^2A'_1/(2a'_1)^{-1}$			
Exp.	17.0 ¹⁷⁷				17.0 ¹⁷⁷				17.0 ¹⁷⁷			
CC2	16.704	16.738	16.866	16.921	12.942	13.081	13.231	13.276	18.210	18.337	18.427	18.465
CCSD	17.256	17.338	17.494	17.553	12.995	13.204	13.342	13.375	18.100	18.300	18.398	18.428
CC3	16.898	16.992	17.102	17.148	12.941	13.191	13.309	13.334	18.018	18.249	18.326	18.349
CCSDT	16.938	17.036	17.156	17.207	12.938	13.189	13.304	13.330	18.002	18.232	18.307	18.331
CC4	16.905	17.005	17.107	×	12.938	13.193	13.306	13.331	18.001	18.236	18.308	18.331
CCSDTQ	16.906	17.005	17.108	×	12.938	13.193	13.307	×	18.001	18.237	18.309	×
FCI	16.901	17.002	17.107	17.156(5)	12.938	13.194	13.307	13.332	18.001	18.238	18.310	18.332
G ₀ W ₀	17.651	17.714	18.015	18.162	13.202	13.395	13.678	13.780	18.320	18.470	18.685	18.780
qsGW	17.463	17.635	17.821	17.909	13.047	13.371	13.584	13.651	18.111	18.410	18.544	18.601
G ₀ F(2)	16.460	16.463	16.656	16.742	12.989	13.093	13.278	13.341	18.255	18.342	18.459	18.515
G ₀ T ₀	17.317	17.298	17.473	×	13.130	13.179	13.327	×	18.536	18.598	18.683	×
Mol.	Formaldehyde (CH ₂ O)				Formaldehyde (CH ₂ O)				Formaldehyde (CH ₂ O)			
State/Conf.	$2^2B_1/(2b_2)^{-1}(2b_1)^1$				$3^2B_2/(1b_1)^{-1}(2b_2)^{-1}(2b_1)^1$				$3^2B_2/(1b_1)^{-1}(2b_2)^{-1}(2b_1)^1$			
Exp.	16.348				16.348				16.348			
CC3	16.564	16.632	16.800	16.847	18.826	18.991	19.154	19.208	×	×	×	×
CCSDT	16.684	16.786	17.004	17.083	18.761	18.956	19.153	19.233	×	×	×	×
CC4	16.348	16.407	16.495	×	18.503	18.663	18.751	×	×	×	×	×
CCSDTQ	16.363	16.425	16.522	×	18.515	18.679	18.772	×	×	×	×	×
FCI	16.345	16.409	16.498(1)	×	18.512	18.678	18.763(1)	×	×	×	×	×
Mol.	Borane (BH ₃)				Borane (BH ₃)				Borane (BH ₃)			
State/Conf.	$1^2B'_1/(1e')^{-2}(1b_1)^1$				$2^2E'/(1e')^{-2}(1b_1)^1$				$2^2E'/(1e')^{-2}(1b_1)^1$			
Exp.	18.754				18.754				18.754			
CC3	19.485	19.803	19.889	19.894	20.026	20.212	20.324	20.346	×	×	×	×
CCSDT	18.896	19.228	19.331	19.355	19.482	19.669	19.789	19.824	×	×	×	×
CC4	18.790	19.130	19.209	19.226	19.403	19.602	19.704	19.732	×	×	×	×
CCSDTQ	18.756	19.100	19.178	×	19.379	19.584	19.684	×	×	×	×	×
FCI	18.754	19.099	19.176	19.194	19.377	19.583	19.685	19.714	×	×	×	×

file for each molecule. This json file contains all the IPs and satellite transition energies of a given molecule as well as the FCI incertitudes and the spectral weight associated with the G_0W_0 , $G_0F(2)$, and G_0T_0 quasiparticle energies.

REFERENCES

- 1T. A. Carlson, *Annu. Rev. Phys. Chem.* **26**, 211 (1975).
- 2S. Hüfner, S. Schmidt, and F. Reinert, *Nucl. Instrum. Methods Phys. Res., Sect. A* **547**, 8 (2005).
- 3C. S. Fadley, *J. Electron Spectrosc. Relat. Phenom.* **178–179**, 2 (2010).
- 4M. J. Campbell, J. Liesegang, J. D. Riley, and J. G. Jenkin, *J. Phys. C: Solid State Phys.* **15**, 2549 (1982).
- 5B. Winter, R. Weber, W. Widdra, M. Dittmar, M. Faubel, and I. V. Hertel, *J. Phys. Chem. A* **108**, 2625 (2004).
- 6R. Seidel, B. Winter, and S. E. Bradforth, *Annu. Rev. Phys. Chem.* **67**, 283 (2016).
- 7T. Buttersack, P. E. Mason, R. S. McMullen, T. Martinek, K. Brezina, D. Hein, H. Ali, C. Kolbeck, C. Schewe, S. Malerz, B. Winter, R. Seidel, O. Marsalek, P. Jungwirth, and S. E. Bradforth, *JACS* **141**, 1838 (2019).
- 8P. Norman and A. Dreuw, *Chem. Rev.* **118**, 7208 (2018).
- 9J. H. Starcke, M. Wormit, J. Schirmer, and A. Dreuw, *Chem. Phys.* **329**, 39 (2006).
- 10P.-F. Loos, M. Boggio-Pasqua, A. Scemama, M. Caffarel, and D. Jacquemin, *J. Chem. Theory Comput.* **15**, 1939 (2019).
- 11M. T. do Casal, J. M. Toldo, M. Barbatti, and F. Plasser, *Chem. Sci.* **14**, 4012 (2023).
- 12L. Cederbaum, *Mol. Phys.* **28**, 479 (1974).
- 13C. Mejuto-Zaera, G. Weng, M. Romanova, S. J. Cotton, K. B. Whaley, N. M. Tubman, and V. Vlček, *J. Chem. Phys.* **154**, 121101 (2021).
- 14J. A. Pople, M. Head-Gordon, D. J. Fox, K. Raghavachari, and L. A. Curtiss, *J. Chem. Phys.* **90**, 5622 (1989).
- 15L. A. Curtiss, K. Raghavachari, G. W. Trucks, and J. A. Pople, *J. Chem. Phys.* **94**, 7221 (1991).
- 16L. A. Curtiss, K. Raghavachari, P. C. Redfern, V. Rassolov, and J. A. Pople, *J. Chem. Phys.* **109**, 7764 (1998).
- 17A. Tajti, P. G. Szalay, A. G. Császár, M. Kállay, J. Gauss, E. F. Valeev, B. A. Flowers, J. Vázquez, and J. F. Stanton, *J. Chem. Phys.* **121**, 11599 (2004).
- 18P. Jurečka, J. Šponer, J. Černý, and P. Hobza, *Phys. Chem. Chem. Phys.* **8**, 1985 (2006).
- 19Y. Zhao and D. G. Truhlar, *J. Chem. Phys.* **124**, 224105 (2006).
- 20M. Schreiber, M. R. Silva-Junior, S. P. A. Sauer, and W. Thiel, *J. Chem. Phys.* **128**, 134110 (2008).
- 21L. Goerigk and S. Grimme, *J. Chem. Theory Comput.* **6**, 107 (2010).
- 22N. Mardirossian and M. Head-Gordon, *Mol. Phys.* **115**, 2315 (2017).
- 23P.-F. Loos, A. Scemama, and D. Jacquemin, *J. Phys. Chem. Lett.* **11**, 2374 (2020).
- 24M. J. van Setten, F. Caruso, S. Sharifzadeh, X. Ren, M. Scheffler, F. Liu, J. Lischner, L. Lin, J. R. Deslippe, S. G. Louie, C. Yang, F. Weigend, J. B. Neaton, F. Evers, and P. Rinke, *J. Chem. Theory Comput.* **11**, 5665 (2015).
- 25F. Caruso, M. Dauth, M. J. van Setten, and P. Rinke, *J. Chem. Theory Comput.* **12**, 5076 (2016).
- 26K. Krause and W. Klopper, *J. Comput. Chem.* **38**, 383 (2017).
- 27L. Gallandi, N. Marom, P. Rinke, and T. Körzdörfer, *J. Chem. Theory Comput.* **12**, 605 (2016).
- 28R. M. Richard, M. S. Marshall, O. Dolgounitcheva, J. V. Ortiz, J.-L. Brédas, N. Marom, and C. D. Sherrill, *J. Chem. Theory Comput.* **12**, 595 (2016).
- 29J. W. Knight, X. Wang, L. Gallandi, O. Dolgounitcheva, X. Ren, J. V. Ortiz, P. Rinke, T. Körzdörfer, and N. Marom, *J. Chem. Theory Comput.* **12**, 615 (2016).
- 30O. Dolgounitcheva, M. Diaz-Tinoco, V. G. Zakrzewski, R. M. Richard, N. Marom, C. D. Sherrill, and J. V. Ortiz, *J. Chem. Theory Comput.* **12**, 627 (2016).
- 31J. Čížek, *J. Chem. Phys.* **45**, 4256 (1966).
- 32G. P. Purvis III and R. J. Bartlett, *J. Chem. Phys.* **76**, 1910 (1982).
- 33K. Raghavachari, G. W. Trucks, J. A. Pople, and M. Head-Gordon, *Chem. Phys. Lett.* **157**, 479 (1989).
- 34I. Shavitt and R. J. Bartlett, *Many-Body Methods in Chemistry and Physics: MBPT and Coupled-Cluster Theory*, Cambridge Molecular Science (Cambridge University Press, Cambridge, 2009).
- 35D. S. Ranasinghe, J. T. Margraf, A. Perera, and R. J. Bartlett, *J. Chem. Phys.* **150**, 074108 (2019).
- 36J. F. Stanton and R. J. Bartlett, *J. Chem. Phys.* **98**, 7029 (1993).
- 37J. D. Watts and R. J. Bartlett, *J. Chem. Phys.* **101**, 3073 (1994).
- 38M. Musiał, S. A. Kucharski, and R. J. Bartlett, *J. Chem. Phys.* **118**, 1128 (2003).
- 39M. Kamiya and S. Hirata, *J. Chem. Phys.* **125**, 074111 (2006).
- 40J. R. Gour and P. Piecuch, *J. Chem. Phys.* **125**, 234107 (2006).
- 41A. Szabo and N. S. Ostlund, *Modern quantum chemistry* (McGraw-Hill, New York, 1989).
- 42J. P. Perdew and M. R. Norman, *Phys. Rev. B* **26**, 5445 (1982).
- 43S. Ivanov, S. Hirata, and R. J. Bartlett, *Phys. Rev. Lett.* **83**, 5455 (1999).
- 44D. P. Chong, O. V. Gritsenko, and E. J. Baerends, *J. Chem. Phys.* **116**, 1760 (2002).
- 45K. Hirao, H.-S. Bae, J.-W. Song, and B. Chan, *J. Phys.: Cond. Mat.* **34**, 194001 (2022).
- 46A. Görling, *Phys. Rev. B* **91**, 245120 (2015).
- 47A. Thierbach, C. Neiss, L. Gallandi, N. Marom, T. Körzdörfer, and A. Görling, *J. Chem. Theory Comput.* **13**, 4726 (2017).
- 48D. Mester and M. Kállay, *J. Chem. Theory Comput.* **19**, 3982 (2023).
- 49P. Verma and R. J. Bartlett, *J. Chem. Phys.* **140**, 18A534 (2014).
- 50Y. Jin and R. J. Bartlett, *J. Chem. Phys.* **145**, 034107 (2016).
- 51Y. Jin and R. J. Bartlett, *J. Chem. Phys.* **149**, 064111 (2018).
- 52P. S. Bagus, *Phys. Rev.* **139**, A619 (1965).
- 53M. Guest and V. Saunders, *Mol. Phys.* **29**, 873 (1975).
- 54N. A. Besley, A. T. B. Gilbert, and P. M. W. Gill, *J. Chem. Phys.* **130**, 124308 (2009).
- 55N. Pueyo Bellafont, G. Álvarez Saiz, F. Viñes, and F. Illas, *Theor. Chem. Acc.* **135**, 35 (2016).
- 56J. V. Jorstad, T. Xie, and C. M. Morales, *Int. J. Quant. Chem.* **122**, e26881 (2022).
- 57J. M. Kalk and J. Lischner, *J. Chem. Theory Comput.* **19**, 3276 (2023).
- 58K. Hirao, T. Nakajima, and B. Chan, *J. Phys. Chem. A* **127**, 7954 (2023).
- 59J. Olsen, P. Jørgensen, H. Koch, A. Balkova, and R. J. Bartlett, *J. Chem. Phys.* **104**, 8007 (1996).
- 60A. L. Dempwolff, M. Hodecker, and A. Dreuw, *J. Chem. Phys.* **156**, 054114 (2022).
- 61K. Krause, M. E. Harding, and W. Klopper, *Mol. Phys.* **113**, 1952 (2015).
- 62X. Zheng and L. Cheng, *J. Chem. Theory Comput.* **15**, 4945 (2019).
- 63J. Lee, D. W. Small, and M. Head-Gordon, *J. Chem. Phys.* **151**, 214103 (2019).
- 64X. Zheng, C. Zhang, Z. Jin, S. H. Southworth, and L. Cheng, *Phys. Chem. Chem. Phys.* **24**, 13587 (2022).
- 65C. F. Bender and E. R. Davidson, *Phys. Rev.* **183**, 23 (1969).
- 66J. L. Whitten and M. Hackmeyer, *J. Chem. Phys.* **51**, 5584 (1969).
- 67B. Huron, J. P. Malrieu, and P. Rancurel, *J. Chem. Phys.* **58**, 5745 (1973).

- ⁶⁸R. J. Buenker and S. D. Peyerimhoff, *Theor. Chim. Acta* **35**, 33 (1974).
- ⁶⁹J. J. Eriksen, T. A. Anderson, J. E. Deustua, K. Ghanem, D. Hait, M. R. Hoffmann, S. Lee, D. S. Levine, I. Magoulas, J. Shen, N. M. Tubman, K. B. Whaley, E. Xu, Y. Yao, N. Zhang, A. Alavi, G. K.-L. Chan, M. Head-Gordon, W. Liu, P. Piecuch, S. Sharma, S. L. Ten-no, C. J. Umrigar, and J. Gauss, *J. Phys. Chem. Lett.* **11**, 8922 (2020).
- ⁷⁰J. J. Eriksen, *J. Phys. Chem. Lett.* **12**, 418 (2021).
- ⁷¹M. Caffarel, T. Applencourt, E. Giner, and A. Scemama, *J. Chem. Phys.* **144**, 151103 (2016).
- ⁷²J. B. Schriber and F. A. Evangelista, *J. Chem. Phys.* **144**, 161106 (2016).
- ⁷³A. A. Holmes, C. J. Umrigar, and S. Sharma, *J. Chem. Phys.* **147**, 164111 (2017).
- ⁷⁴Y. Damour, M. V eril, F. Kossoski, M. Caffarel, D. Jacquemin, A. Scemama, and P.-F. Loos, *J. Chem. Phys.* **155**, 134104 (2021).
- ⁷⁵H. R. Larsson, H. Zhai, C. J. Umrigar, and G. K.-L. Chan, *J. Am. Chem. Soc.* **144**, 15932 (2022).
- ⁷⁶N. M. Tubman, J. Lee, T. Y. Takeshita, M. Head-Gordon, and K. B. Whaley, *J. Chem. Phys.* **145**, 044112 (2016).
- ⁷⁷N. M. Tubman, D. S. Levine, D. Hait, M. Head-Gordon, and K. B. Whaley, *arXiv* (2018), 10.48550/arXiv.1808.02049, 1808.02049.
- ⁷⁸N. M. Tubman, C. D. Freeman, D. S. Levine, D. Hait, M. Head-Gordon, and K. B. Whaley, *J. Chem. Theory Comput.* **16**, 2139 (2020).
- ⁷⁹R. M. Martin, L. Reining, and D. M. Ceperley, *Interacting Electrons: Theory and Computational Approaches* (Cambridge University Press, 2016).
- ⁸⁰D. Golze, M. Dvorak, and P. Rinke, *Front. Chem.* **7**, 377 (2019).
- ⁸¹A. Marie, A. Ammar, and P.-F. Loos, "The GW Approximation: A Quantum Chemistry Perspective," (2023), arxiv:2311.05351.
- ⁸²J. Schirmer, *Many-Body Methods for Atoms, Molecules and Clusters* (Springer, 2018).
- ⁸³S. Banerjee and A. Y. Sokolov, *J. Chem. Theory Comput.* **19**, 3037 (2023).
- ⁸⁴G. Strinati, H. J. Mattausch, and W. Hanke, *Phys. Rev. Lett.* **45**, 290 (1980).
- ⁸⁵M. S. Hybertsen and S. G. Louie, *Phys. Rev. Lett.* **55**, 1418 (1985).
- ⁸⁶R. W. Godby, M. Schl uter, and L. J. Sham, *Phys. Rev. B* **37**, 10159 (1988).
- ⁸⁷W. von der Linden and P. Horsch, *Phys. Rev. B* **37**, 8351 (1988).
- ⁸⁸J. E. Northrup, M. S. Hybertsen, and S. G. Louie, *Phys. Rev. Lett.* **66**, 500 (1991).
- ⁸⁹X. Blase, X. Zhu, and S. G. Louie, *Phys. Rev. B* **49**, 4973 (1994).
- ⁹⁰M. Rohlfing, P. Kr uger, and J. Pollmann, *Phys. Rev. B* **52**, 1905 (1995).
- ⁹¹D. Neuhauser, E. Rabani, and R. Baer, *J. Phys. Chem. Lett.* **4**, 1172 (2013).
- ⁹²D. Neuhauser, Y. Gao, C. Arntsen, C. Karshenas, E. Rabani, and R. Baer, *Phys. Rev. Lett.* **113** (2014), 10.1103/PhysRevLett.113.076402.
- ⁹³M. Govoni and G. Galli, *J. Chem. Theory Comput.* **11**, 2680 (2015).
- ⁹⁴V. Vl cek, E. Rabani, D. Neuhauser, and R. Baer, *J. Chem. Theory Comput.* **13**, 4997 (2017).
- ⁹⁵J. Wilhelm, D. Golze, L. Talirz, J. Hutter, and C. A. Pignedoli, *J. Phys. Chem. Lett.* **9**, 306 (2018).
- ⁹⁶I. Duchemin and X. Blase, *J. Chem. Phys.* **150**, 174120 (2019).
- ⁹⁷M. D. Ben, F. H. da Jornada, A. Canning, N. Wichmann, K. Raman, R. Sasanka, C. Yang, S. G. Louie, and J. Deslippe, *Comp. Phys. Comm.* **235**, 187 (2019).
- ⁹⁸A. F orster and L. Visscher, *J. Chem. Theory Comput.* **16**, 7381 (2020).
- ⁹⁹A. F orster and L. Visscher, *Front. Chem.* **9**, 736591 (2021).
- ¹⁰⁰I. Duchemin and X. Blase, *J. Chem. Theory Comput.* **16**, 1742 (2020).
- ¹⁰¹I. Duchemin and X. Blase, *J. Chem. Theory Comput.* **17**, 2383 (2021).
- ¹⁰²A. F orster and L. Visscher, *J. Chem. Theory Comput.* **18**, 6779 (2022).
- ¹⁰³R. L. Panad es-Barrueta and D. Golze, *J. Chem. Theory Comput.* **19**, 5450 (2023).
- ¹⁰⁴M. Shishkin and G. Kresse, *Phys. Rev. B* **75**, 235102 (2007).
- ¹⁰⁵X. Blase, C. Attaccalite, and V. Olevano, *Phys. Rev. B* **83**, 115103 (2011).
- ¹⁰⁶N. Marom, F. Caruso, X. Ren, O. T. Hofmann, T. K orzd orfer, J. R. Chelikowsky, A. Rubio, M. Scheffler, and P. Rinke, *Phys. Rev. B* **86**, 245127 (2012).
- ¹⁰⁷J. Wilhelm, M. Del Ben, and J. Hutter, *J. Chem. Theory Comput.* **12**, 3623 (2016).
- ¹⁰⁸F. Kaplan, M. E. Harding, C. Seiler, F. Weigend, F. Evers, and M. J. van Setten, *J. Chem. Theory Comput.* **12**, 2528 (2016).
- ¹⁰⁹S. V. Faleev, M. van Schilfgaarde, and T. Kotani, *Phys. Rev. Lett.* **93**, 126406 (2004).
- ¹¹⁰M. van Schilfgaarde, T. Kotani, and S. Faleev, *Phys. Rev. Lett.* **96**, 226402 (2006).
- ¹¹¹T. Kotani, M. van Schilfgaarde, and S. V. Faleev, *Phys. Rev. B* **76**, 165106 (2007).
- ¹¹²S.-H. Ke, *Phys. Rev. B* **84**, 205415 (2011).
- ¹¹³A. Marie and P.-F. Loos, *J. Chem. Theory Comput.* **19**, 3943 (2023).
- ¹¹⁴M. E. Casida and D. P. Chong, *Phys. Rev. A* **40**, 4837 (1989).
- ¹¹⁵M. E. Casida and D. P. Chong, *Phys. Rev. A* **44**, 5773 (1991).
- ¹¹⁶G. Stefanucci and R. van Leeuwen, *Nonequilibrium Many-Body Theory of Quantum Systems: A Modern Introduction* (Cambridge University Press, Cambridge, 2013).
- ¹¹⁷J. V. Ortiz, *Wiley Interdiscip. Rev. Comput. Mol. Sci.* **3**, 123 (2013).
- ¹¹⁸J. J. Phillips and D. Zgid, *J. Chem. Phys.* **140**, 241101 (2014).
- ¹¹⁹J. J. Phillips, A. A. Kananenka, and D. Zgid, *J. Chem. Phys.* **142**, 194108 (2015).
- ¹²⁰A. A. Rusakov, J. J. Phillips, and D. Zgid, *J. Chem. Phys.* **141**, 194105 (2014).
- ¹²¹A. A. Rusakov and D. Zgid, *J. Chem. Phys.* **144**, 054106 (2016).
- ¹²²S. Hirata, M. R. Hermes, J. Simons, and J. V. Ortiz, *J. Chem. Theory Comput.* **11**, 1595 (2015).
- ¹²³S. Hirata, A. E. Doran, P. J. Knowles, and J. V. Ortiz, *J. Chem. Phys.* **147**, 044108 (2017).
- ¹²⁴O. J. Backhouse, A. Santana-Bonilla, and G. H. Booth, *J. Phys. Chem. Lett.* **12**, 7650 (2021).
- ¹²⁵O. J. Backhouse and G. H. Booth, *J. Chem. Theory Comput.* **16**, 6294 (2020).
- ¹²⁶O. J. Backhouse, M. Nusspickel, and G. H. Booth, *J. Chem. Theory Comput.* **16**, 1090 (2020).
- ¹²⁷P. Pokhilko and D. Zgid, *J. Chem. Phys.* **155**, 024101 (2021).
- ¹²⁸P. Pokhilko, S. Isakov, C.-N. Yeh, and D. Zgid, *J. Chem. Phys.* **155**, 024119 (2021).
- ¹²⁹P. Pokhilko, C.-N. Yeh, and D. Zgid, *J. Chem. Phys.* **156**, 094101 (2022).
- ¹³⁰A. Liebsch, *Phys. Rev. B* **23**, 5203 (1981).
- ¹³¹N. E. Bickers, D. J. Scalapino, and S. R. White, *Phys. Rev. Lett.* **62**, 961 (1989).
- ¹³²N. E. Bickers and S. R. White, *Phys. Rev. B* **43**, 8044 (1991).
- ¹³³M. I. Katsnelson and A. I. Lichtenstein, *J. Phys. Condens. Matter* **11**, 1037 (1999).
- ¹³⁴M. Katsnelson and A. Lichtenstein, *Eur. Phys. J. B* **30**, 9 (2002).
- ¹³⁵V. P. Zhukov, E. V. Chulkov, and P. M. Echenique, *Phys. Rev. B* **72**, 72.155109 (2005).
- ¹³⁶M. Puig von Friesen, C. Verdozzi, and C.-O. Almbladh, *Phys. Rev. B* **82**, 155108 (2010).
- ¹³⁷P. Romaniello, F. Bechstedt, and L. Reining, *Phys. Rev. B* **85**, 155131 (2012).
- ¹³⁸J. Gukelberger, L. Huang, and P. Werner, *Phys. Rev. B* **91**, 235114 (2015).
- ¹³⁹M. C. T. D. M uller, S. Bl ugel, and C. Friedrich, *Phys. Rev. B* **100**, 045130 (2019).

- ¹⁴⁰C. Friedrich, *Phys. Rev. B* **100**, 075142 (2019).
- ¹⁴¹T. Biswas and A. Singh, *npj Comput. Mater.* **7**, 189 (2021).
- ¹⁴²D. Zhang, N. Q. Su, and W. Yang, *J. Phys. Chem. Lett.* **8**, 3223 (2017).
- ¹⁴³J. Li, Z. Chen, and W. Yang, *J. Phys. Chem. Lett.* **12**, 6203 (2021).
- ¹⁴⁴J. Li, J. Yu, Z. Chen, and W. Yang, *J. Phys. Chem. A* **127**, 7811 (2023).
- ¹⁴⁵P.-F. Loos and P. Romaniello, *J. Chem. Phys.* **156**, 164101 (2022).
- ¹⁴⁶R. Orlando, P. Romaniello, and P.-F. Loos, “Exploring new exchange-correlation kernels in the bethe–salpeter equation: A study of the asymmetric hubbard dimer,” in *Advances in Quantum Chemistry* (Elsevier, 2023) pp. 183–211.
- ¹⁴⁷R. Orlando, P. Romaniello, and P.-F. Loos, *J. Chem. Phys.* **159**, 184113 (2023).
- ¹⁴⁸A. M. Lewis and T. C. Berkelbach, *J. Chem. Theory Comput.* **15**, 2925 (2019).
- ¹⁴⁹F. Bruneval, N. Dattani, and M. J. van Setten, *Front. Chem.* **9**, 749779 (2021).
- ¹⁵⁰E. Monino and P.-F. Loos, *J. Chem. Phys.* **159**, 034105 (2023).
- ¹⁵¹G. Baym and L. P. Kadanoff, *Phys. Rev.* **124**, 287 (1961).
- ¹⁵²G. Baym, *Phys. Rev.* **127**, 1391 (1962).
- ¹⁵³C. De Dominicis and P. C. Martin, *J. Math. Phys.* **5**, 14 (1964).
- ¹⁵⁴C. De Dominicis and P. C. Martin, *J. Math. Phys.* **5**, 31 (1964).
- ¹⁵⁵N. Bickers and D. Scalapino, *Ann. Phys.* **193**, 206 (1989).
- ¹⁵⁶L. Hedin, *J. Phys. Condens. Matter* **11**, R489 (1999).
- ¹⁵⁷N. E. Bickers, “Self-consistent many-body theory for condensed matter systems,” in *Theoretical Methods for Strongly Correlated Electrons*, edited by D. Sénéchal, A.-M. Tremblay, and C. Bourbonnais (Springer New York, New York, NY, 2004) pp. 237–296.
- ¹⁵⁸E. L. Shirley, *Phys. Rev. B* **54**, 7758 (1996).
- ¹⁵⁹R. Del Sole, L. Reining, and R. W. Godby, *Phys. Rev. B* **49**, 8024 (1994).
- ¹⁶⁰A. Schindlmayr and R. W. Godby, *Phys. Rev. Lett.* **80**, 1702 (1998).
- ¹⁶¹A. J. Morris, M. Stankovski, K. T. Delaney, P. Rinke, P. García-González, and R. W. Godby, *Phys. Rev. B* **76**, 155106 (2007).
- ¹⁶²M. Shishkin, M. Marsman, and G. Kresse, *Phys. Rev. Lett.* **99**, 246403 (2007).
- ¹⁶³P. Romaniello, S. Guyot, and L. Reining, *J. Chem. Phys.* **131**, 154111 (2009).
- ¹⁶⁴A. Grüneis, G. Kresse, Y. Hinuma, and F. Oba, *Phys. Rev. Lett.* **112**, 096401 (2014).
- ¹⁶⁵L. Hung, F. Bruneval, K. Baishya, and S. Ögüt, *J. Chem. Theory Comput.* **13**, 2135 (2017).
- ¹⁶⁶E. Maggio and G. Kresse, *J. Chem. Theory Comput.* **13**, 4765 (2017).
- ¹⁶⁷C. Mejuto-Zaera and V. c. v. Vlček, *Phys. Rev. B* **106**, 165129 (2022).
- ¹⁶⁸M. Wen, V. Abraham, G. Harsha, A. Shee, B. Whaley, and D. Zgid, “Comparing self-consistent GW and vertex corrected G0W0 accuracy for molecular ionization potentials,” (2023), arxiv:2311.12209.
- ¹⁶⁹J. Schirmer, L. S. Cederbaum, W. Domcke, and W. von Niessen, *Chem. Phys.* **26**, 149 (1977).
- ¹⁷⁰L. S. Cederbaum, J. Schirmer, W. Domcke, and W. von Niessen, *J. Phys. B: At. Mol. Phys.* **10**, L549 (1977).
- ¹⁷¹J. Schirmer and L. S. Cederbaum, *J. Phys. B: At. Mol. Phys.* **11**, 1889 (1978).
- ¹⁷²J. Schirmer, W. Domcke, L. S. Cederbaum, and W. von Niessen, *J. Phys. B: At. Mol. Phys.* **11**, 1901 (1978).
- ¹⁷³J. Schirmer, L. S. Cederbaum, W. Domcke, and W. Von Niessen, *Chem. Phys. Lett.* **57**, 582 (1978).
- ¹⁷⁴W. Domcke, L. S. Cederbaum, J. Schirmer, W. von Niessen, and J. P. Maier, *J. Electron Spectrosc. Relat. Phenom.* **14**, 59 (1978).
- ¹⁷⁵L. S. Cederbaum, J. Schirmer, W. Domcke, and W. Von Niessen, *Int. J. Quantum Chem.* **14**, 593 (1978).
- ¹⁷⁶L. S. Cederbaum, W. Domcke, J. Schirmer, and W. von Niessen, *Phys. Scr.* **21**, 481 (1980).
- ¹⁷⁷W. von Niessen, G. Bieri, and L. Åsbrink, *J. Electron Spectrosc. Relat. Phenom.* **21**, 175 (1980).
- ¹⁷⁸W. Von Niessen, L. S. Cederbaum, W. Domcke, and G. H. F. Diercksen, *Chem. Phys.* **56**, 43 (1981).
- ¹⁷⁹O. Walter and J. Schirmer, *J. Phys. B: At. Mol. Phys.* **14**, 3805 (1981).
- ¹⁸⁰J. Schirmer and O. Walter, *Chem. Phys.* **78**, 201 (1983).
- ¹⁸¹L. S. Cederbaum, W. Domcke, J. Schirmer, and W. V. Niessen, in *Adv. Chem. Phys.* (1986) pp. 115–159.
- ¹⁸²P. S. Bagus and E.-K. Viinikka, *Phys. Rev. A* **15**, 1486 (1977).
- ¹⁸³N. Kosugi, H. Kuroda, and S. Iwata, *Chem. Phys.* **39**, 337 (1979).
- ¹⁸⁴N. Kosugi, H. Kuroda, and S. Iwata, *Chem. Phys.* **58**, 267 (1981).
- ¹⁸⁵N. Honjou, T. Sasajima, and F. Sasaki, *Chem. Phys.* **57**, 475 (1981).
- ¹⁸⁶H. Nakatsuji and T. Yonezawa, *Chem. Phys. Lett.* **87**, 426 (1982).
- ¹⁸⁷R. Arneberg, *Chem. Phys.* **64**, 249 (1982).
- ¹⁸⁸P. Roy, I. Nenner, P. Millie, P. Morin, and D. Roy, *J. Chem. Phys.* **84**, 2050 (1986).
- ¹⁸⁹A. O. Bawagan, R. Müller-Fiedler, C. E. Brion, E. R. Davidson, and C. Boyle, *Chem. Phys.* **120**, 335 (1988).
- ¹⁹⁰A. O. Bawagan, C. E. Brion, E. R. Davidson, C. Boyle, and R. F. Frey, *Chem. Phys.* **128**, 439 (1988).
- ¹⁹¹S. A. C. Clark, C. E. Brion, E. R. Davidson, and C. Boyle, *Chem. Phys.* **136**, 55 (1989).
- ¹⁹²S. A. C. Clark, T. J. Reddish, C. E. Brion, E. R. Davidson, and R. F. Frey, *Chem. Phys.* **143**, 1 (1990).
- ¹⁹³A. Lisini, P. Decleva, and G. Fronzoni, *J. Mol. Struct. THEOCHEM* **228**, 97 (1991).
- ¹⁹⁴H. Nakatsuji, *Chem. Phys.* **75**, 425 (1983).
- ¹⁹⁵H. Wasada and K. Hirao, *Chem. Phys.* **138**, 277 (1989).
- ¹⁹⁶H. Nakatsuji, *Chem. Phys. Lett.* **177**, 331 (1991).
- ¹⁹⁷M. Ehara and H. Nakatsuji, *Chem. Phys. Lett.* **282**, 347 (1998).
- ¹⁹⁸M. Ehara and H. Nakatsuji, *Spectrochim. Acta., Part A* **55**, 487 (1999).
- ¹⁹⁹M. Ehara, P. Tomasello, J. Hasegawa, and H. Nakatsuji, *Theor. Chem. Acc.* **102**, 161 (1999).
- ²⁰⁰M. Ehara, M. Ishida, and H. Nakatsuji, *J. Chem. Phys.* **114**, 8990 (2001).
- ²⁰¹M. Ishida, M. Ehara, and H. Nakatsuji, *J. Chem. Phys.* **116**, 1934 (2002).
- ²⁰²M. Ehara, S. Yasuda, and H. Nakatsuji, *Z. Phys. Chem.* **217**, 161 (2003).
- ²⁰³Y. Ohtsuka and H. Nakatsuji, *J. Chem. Phys.* **124**, 054110 (2006).
- ²⁰⁴C. G. Ning, B. Hajgató, Y. R. Huang, S. F. Zhang, K. Liu, Z. H. Luo, S. Knippenberg, J. K. Deng, and M. S. Deleuze, *Chem. Phys.* **343**, 19 (2008).
- ²⁰⁵Q. Tian, J. Yang, Y. Shi, X. Shan, and X. Chen, *J. Chem. Phys.* **136**, 094306 (2012).
- ²⁰⁶F. Aryasetiawan, L. Hedin, and K. Karlsson, *Phys. Rev. Lett.* **77**, 2268 (1996).
- ²⁰⁷M. Vos, A. S. Kheifets, E. Weigold, and F. Aryasetiawan, *Phys. Rev. B* **63**, 033108 (2001).
- ²⁰⁸M. Vos, A. Kheifets, V. Sashin, E. Weigold, M. Usuda, and F. Aryasetiawan, *Phys. Rev. B* **66**, 155414 (2002).
- ²⁰⁹A. S. Kheifets, V. A. Sashin, M. Vos, E. Weigold, and F. Aryasetiawan, *Phys. Rev. B* **68**, 233205 (2003).
- ²¹⁰M. Guzzo, G. Lani, F. Sottile, P. Romaniello, M. Gatti, J. J. Kas, J. J. Rehr, M. G. Silly, F. Sirotti, and L. Reining, *Phys. Rev. Lett.* **107**, 166401 (2011).
- ²¹¹M. Guzzo, J. J. Kas, L. Sponza, C. Giorgetti, F. Sottile, D. Pierucci, M. G. Silly, F. Sirotti, J. J. Rehr, and L. Reining, *Phys. Rev. B* **89**, 085425 (2014).
- ²¹²J. Lischner, D. Vigil-Fowler, and S. G. Louie, *Phys. Rev. Lett.* **110**, 146801 (2013).
- ²¹³J. S. Zhou, J. J. Kas, L. Sponza, I. Reshetnyak, M. Guzzo, C. Giorgetti, M. Gatti, F. Sottile, J. J. Rehr, and L. Reining, *J.*

- Chem. Phys.* **143**, 184109 (2015).
- ²¹⁴D. Vigil-Fowler, S. G. Louie, and J. Lischner, *Phys. Rev. B* **93**, 235446 (2016).
- ²¹⁵V. Vlček, E. Rabani, and D. Neuhauser, *Phys. Rev. Materials* **2**, 030801 (2018).
- ²¹⁶B. Holm and F. Aryasetiawan, *Phys. Rev. B* **56**, 12825 (1997).
- ²¹⁷B. Holm and F. Aryasetiawan, *Phys. Rev. B* **62**, 4858 (2000).
- ²¹⁸J. Lischner, D. Vigil-Fowler, and S. G. Louie, *Phys. Rev. B* **89**, 125430 (2014).
- ²¹⁹J. J. Kas, J. J. Rehr, and L. Reining, *Phys. Rev. B* **90**, 085112 (2014).
- ²²⁰J. McClain, J. Lischner, T. Watson, D. A. Matthews, E. Ronca, S. G. Louie, T. C. Berkelbach, and G. K.-L. Chan, *Phys. Rev. B* **93**, 235139 (2016).
- ²²¹J. J. Kas, F. D. Vila, T. S. Tan, and J. J. Rehr, *Electron. Struct.* **4**, 033001 (2022).
- ²²²M. Z. Mayers, M. S. Hybertsen, and D. R. Reichman, *Phys. Rev. B* **94**, 081109 (2016).
- ²²³J. S. Zhou, M. Gatti, J. J. Kas, J. J. Rehr, and L. Reining, *Phys. Rev. B* **97**, 035137 (2018).
- ²²⁴M. Tzavala, J. J. Kas, L. Reining, and J. J. Rehr, *Phys. Rev. Research* **2**, 033147 (2020).
- ²²⁵B. I. Lundqvist, *Phys kondens Materie* **9**, 236 (1969).
- ²²⁶D. C. Langreth, *Phys. Rev. B* **1**, 471 (1970).
- ²²⁷L. Hedin, *Phys. Scr.* **21**, 477 (1980).
- ²²⁸Y. Garniron, A. Scemama, E. Giner, M. Caffarel, and P. F. Loos, *J. Chem. Phys.* **149**, 064103 (2018).
- ²²⁹A. D. Chien, A. A. Holmes, M. Otten, C. J. Umrigar, S. Sharma, and P. M. Zimmerman, *J. Phys. Chem. A* **122**, 2714 (2018).
- ²³⁰P. F. Loos, A. Scemama, A. Blondel, Y. Garniron, M. Caffarel, and D. Jacquemin, *J. Chem. Theory Comput.* **14**, 4360 (2018).
- ²³¹P. F. Loos, F. Lipparini, M. Boggio-Pasqua, A. Scemama, and D. Jacquemin, *J. Chem. Theory Comput.* **16**, 1711 (2020).
- ²³²A. A. Holmes, N. M. Tubman, and C. J. Umrigar, *J. Chem. Theory Comput.* **12**, 3674 (2016).
- ²³³S. Sharma, A. A. Holmes, G. Jeanmairet, A. Alavi, and C. J. Umrigar, *J. Chem. Theory Comput.* **13**, 1595 (2017).
- ²³⁴K. Chatterjee and A. Y. Sokolov, *J. Chem. Theory Comput.* **15**, 5908 (2019).
- ²³⁵K. Chatterjee and A. Y. Sokolov, *J. Chem. Theory Comput.* **16**, 6343 (2020).
- ²³⁶P.-F. Loos, M. Boggio-Pasqua, A. Scemama, M. Caffarel, and D. Jacquemin, *J. Chem. Theory Comput.* **15**, 1939 (2019), <https://doi.org/10.1021/acs.jctc.8b01205>.
- ²³⁷P.-F. Loos, A. Scemama, M. Boggio-Pasqua, and D. Jacquemin, *J. Chem. Theory Comput.* **16**, 3720 (2020).
- ²³⁸M. Véril, A. Scemama, M. Caffarel, F. Lipparini, M. Boggio-Pasqua, D. Jacquemin, and P.-F. Loos, *WIREs Comput. Mol. Sci.* **11**, e1517.
- ²³⁹P.-F. Loos, M. Comin, X. Blase, and D. Jacquemin, *J. Chem. Theory Comput.* **17**, 3666 (2021).
- ²⁴⁰P.-F. Loos, F. Lipparini, D. A. Matthews, A. Blondel, and D. Jacquemin, *J. Chem. Theory Comput.* **18**, 4418 (2022).
- ²⁴¹D. Jacquemin, F. Kossoski, F. Gam, M. Boggio-Pasqua, and P.-F. Loos, *J. Chem. Theory Comput.* **19**, 8782 (2023).
- ²⁴²P.-F. Loos, F. Lipparini, and D. Jacquemin, *J. Phys. Chem. Lett.* **14**, 11069 (2023).
- ²⁴³P.-F. Loos and D. Jacquemin, “A mountaineering strategy to excited states: Accurate vertical transition energies and benchmarks for substituted benzenes,” (2024), [arXiv:2401.13809](https://arxiv.org/abs/2401.13809) [physics.chem-ph].
- ²⁴⁴D. A. Matthews, L. Cheng, M. E. Harding, F. Lipparini, S. Stopkowicz, T.-C. Jagau, P. G. Szalay, J. Gauss, and J. F. Stanton, *J. Chem. Phys.* **152**, 214108 (2020).
- ²⁴⁵O. Christiansen, H. Koch, and P. Jørgensen, *J. Chem. Phys.* **103**, 7429 (1995).
- ²⁴⁶H. Koch, O. Christiansen, P. Jørgensen, A. M. Sanchez de Merás, and T. Helgaker, *J. Chem. Phys.* **106**, 1808 (1997).
- ²⁴⁷M. S. Gordon, J. S. Binkley, J. A. Pople, W. J. Pietro, and W. J. Hehre, *JACS* **104**, 2797 (1982).
- ²⁴⁸M. M. Francl, W. J. Pietro, W. J. Hehre, J. S. Binkley, M. S. Gordon, D. J. DeFrees, and J. A. Pople, *J. Chem. Phys.* **77**, 3654 (1982).
- ²⁴⁹T. Clark, J. Chandrasekhar, G. W. Spitznagel, and P. V. R. Schleyer, *J. Comp. Chem.* **4**, 294 (1983).
- ²⁵⁰R. Ditchfield, W. J. Hehre, and J. A. Pople, *J. Chem. Phys.* **54**, 724 (2003).
- ²⁵¹W. J. Hehre, R. Ditchfield, and J. A. Pople, *J. Chem. Phys.* **56**, 2257 (2003).
- ²⁵²J. D. Dill and J. A. Pople, *J. Chem. Phys.* **62**, 2921 (2008).
- ²⁵³J. S. Binkley and J. A. Pople, *J. Chem. Phys.* **66**, 879 (2008).
- ²⁵⁴T. H. Dunning, Jr., *J. Chem. Phys.* **90**, 1007 (1989).
- ²⁵⁵R. A. Kendall, T. H. Dunning, Jr., and R. J. Harrison, *J. Chem. Phys.* **96**, 6796 (1992).
- ²⁵⁶B. P. Prascher, D. E. Woon, K. A. Peterson, T. H. Dunning, and A. K. Wilson, *Theor. Chem. Acc.* **128**, 69 (2011).
- ²⁵⁷D. E. Woon and T. H. Dunning, Jr., *J. Chem. Phys.* **98**, 1358 (1993).
- ²⁵⁸E. Giner, A. Scemama, and M. Caffarel, *Can. J. Chem.* **91**, 879 (2013).
- ²⁵⁹E. Giner, A. Scemama, and M. Caffarel, *J. Chem. Phys.* **142**, 044115 (2015).
- ²⁶⁰M. Caffarel, T. Applencourt, E. Giner, and A. Scemama, “Using cipsi nodes in diffusion monte carlo,” in *Recent Progress in Quantum Monte Carlo* (2016) Chap. 2, pp. 15–46.
- ²⁶¹Y. Garniron, A. Scemama, P.-F. Loos, and M. Caffarel, *J. Chem. Phys.* **147**, 034101 (2017).
- ²⁶²Y. Garniron, K. Gasperich, T. Applencourt, A. Benali, A. Ferté, J. Paquier, B. Pradines, R. Assaraf, P. Reinhardt, J. Toulouse, P. Barbareco, N. Renon, G. David, J. P. Malrieu, M. Véril, M. Caffarel, P. F. Loos, E. Giner, and A. Scemama, *J. Chem. Theory Comput.* **15**, 3591 (2019).
- ²⁶³M. J. Frisch, G. W. Trucks, H. B. Schlegel, G. E. Scuseria, M. A. Robb, J. R. Cheeseman, G. Scalmani, V. Barone, G. A. Petersson, H. Nakatsuji, X. Li, M. Caricato, A. V. Marenich, J. Bloino, B. G. Janesko, R. Gomperts, B. Mennucci, H. P. Hratchian, J. V. Ortiz, A. F. Izmaylov, J. L. Sonnenberg, D. Williams-Young, F. Ding, F. Lipparini, F. Egidi, J. Goings, B. Peng, A. Petrone, T. Henderson, D. Ranasinghe, V. G. Zakrzewski, J. Gao, N. Rega, G. Zheng, W. Liang, M. Hada, M. Ehara, K. Toyota, R. Fukuda, J. Hasegawa, M. Ishida, T. Nakajima, Y. Honda, O. Kitao, H. Nakai, T. Vreven, K. Throssell, J. A. Montgomery, Jr., J. E. Peralta, F. Ogliaro, M. J. Bearpark, J. J. Heyd, E. N. Brothers, K. N. Kudin, V. N. Staroverov, T. A. Keith, R. Kobayashi, J. Normand, K. Raghavachari, A. P. Rendell, J. C. Burant, S. S. Iyengar, J. Tomasi, M. Cossi, J. M. Millam, M. Klene, C. Adamo, R. Cammi, J. W. Ochterski, R. L. Martin, K. Morokuma, O. Farkas, J. B. Foresman, and D. J. Fox, “GaussianTM 16 Revision C.01,” (2016), gaussian Inc. Wallingford CT.
- ²⁶⁴Y. Damour, R. Quintero-Monsebaiz, M. Caffarel, D. Jacquemin, F. Kossoski, A. Scemama, and P.-F. Loos, *J. Chem. Theory Comput.* **19**, 221 (2023).
- ²⁶⁵H. G. A. Burton and P.-F. Loos, “Rationale for the Extrapolation Procedure in Selected Configuration Interaction,” (2023), [arxiv:2312.12530](https://arxiv.org/abs/2312.12530).
- ²⁶⁶W. R. Inc., “*Mathematica, Version 13.3*,” Champaign, IL, 2023.
- ²⁶⁷G. E. Scuseria, A. C. Scheiner, T. J. Lee, J. E. Rice, and H. F. Schaefer, *J. Chem. Phys.* **86**, 2881 (1987).
- ²⁶⁸H. Koch, H. J. A. Jensen, P. Jørgensen, and T. Helgaker, *J. Chem. Phys.* **93**, 3345 (1990).
- ²⁶⁹H. Koch and P. Jørgensen, *J. Chem. Phys.* **93**, 3333 (1990).
- ²⁷⁰J. F. Stanton, *J. Chem. Phys.* **99**, 8840 (1993).
- ²⁷¹J. Noga and R. J. Bartlett, *J. Chem. Phys.* **86**, 7041 (1987).
- ²⁷²G. E. Scuseria and H. F. Schaefer, *Chem. Phys. Lett.* **152**, 382 (1988).
- ²⁷³S. A. Kucharski, M. Włoch, M. Musiał, and R. J. Bartlett, *J. Chem. Phys.* **115**, 8263 (2001).
- ²⁷⁴S. A. Kucharski and R. J. Bartlett, *Theor. Chim. Acta* **80**, 387 (1991).

- 275 M. Kállay and P. R. Surján, *J. Chem. Phys.* **115**, 2945 (2001).
- 276 S. Hirata, *J. Chem. Phys.* **121**, 51 (2004).
- 277 M. Kállay, J. Gauss, and P. G. Szalay, *J. Chem. Phys.* **119**, 2991 (2003).
- 278 M. Kállay and J. Gauss, *J. Chem. Phys.* **120**, 6841 (2004).
- 279 M. Nooijen and R. J. Bartlett, *J. Chem. Phys.* **102**, 3629 (1995).
- 280 V. Rishi, A. Perera, and R. J. Bartlett, *J. Chem. Phys.* **153**, 234101 (2020).
- 281 R. Quintero-Monsebaiz, E. Monino, A. Marie, and P.-F. Loos, *J. Chem. Phys.* **157**, 231102 (2022).
- 282 J. Tölle and G. Kin-Lic Chan, *J. Chem. Phys.* **158**, 124123 (2023).
- 283 O. Christiansen, H. Koch, and P. Jørgensen, *Chem. Phys. Lett.* **243**, 409 (1995).
- 284 C. Hättig and F. Weigend, *J. Chem. Phys.* **113**, 5154 (2000).
- 285 H. Koch, O. Christiansen, P. Jørgensen, and J. Olsen, *Chem. Phys. Lett.* **244**, 75 (1995).
- 286 K. Hald, P. Jørgensen, J. Olsen, and M. Jaszuński, *J. Chem. Phys.* **115**, 671 (2001).
- 287 A. C. Paul, R. H. Myhre, and H. Koch, *J. Chem. Theory Comput.* **17**, 117 (2021).
- 288 M. Kállay and J. Gauss, *J. Chem. Phys.* **121**, 9257 (2004).
- 289 M. Kállay and J. Gauss, *J. Chem. Phys.* **123**, 214105 (2005).
- 290 P.-F. Loos, D. A. Matthews, F. Lipparini, and D. Jacquemin, *J. Chem. Phys.* **154**, 221103 (2021).
- 291 D. J. Rowe, *Rev. Mod. Phys.* **40**, 153 (1968).
- 292 K. Emrich, *Nuc. Phys. A* **351**, 379 (1981).
- 293 H. Sekino and R. J. Bartlett, *Int. J. Quantum Chem.* **26**, 255 (1984).
- 294 J. Geertsen, M. Rittby, and R. J. Bartlett, *Chem. Phys. Lett.* **164**, 57 (1989).
- 295 D. C. Comeau and R. J. Bartlett, *Chem. Phys. Lett.* **207**, 414 (1993).
- 296 J. F. Stanton and J. Gauss, *J. Chem. Phys.* **111**, 8785 (1999).
- 297 P. F. Loos, “QuAcK: a software for emerging quantum electronic structure methods,” (2019), <https://github.com/pfloos/QuAcK>.
- 298 M. F. Lange and T. C. Berkelbach, *J. Chem. Theory Comput.* **14**, 4224 (2018).
- 299 H.-J. Werner, P. J. Knowles, F. R. Manby, J. A. Black, K. Doll, A. Heßelmann, D. Kats, A. Köhn, T. Korona, D. A. Kreplin, Q. Ma, T. F. Miller, III, A. Mitrushchenkov, K. A. Peterson, I. Polyak, G. Rauhut, and M. Sibaev, *J. Chem. Phys.* **152**, 144107 (2020).
- 300 D. Edvardsson, P. Baltzer, L. Karlsson, B. Wannberg, D. M. P. Holland, D. A. Shaw, and E. E. Rennie, *J. Phys. B: At. Mol. Phys.* **32**, 2583 (1999).
- 301 M. C. Göthe, B. Wannberg, L. Karlsson, S. Svensson, P. Baltzer, F. T. Chau, and M.-Y. Adam, *J. Chem. Phys.* **94**, 2536 (1991).
- 302 G. Bieri, A. Schmelzer, L. Åsbrink, and M. Jonsson, *Chem. Phys.* **49**, 213 (1980).
- 303 S. Svensson, B. Eriksson, N. Mårtensson, G. Wendin, and U. Gelius, *J. Electron Spectrosc. Relat. Phenom.* **47**, 327 (1988).
- 304 R. Cambi, G. Ciullo, A. Sgamellotti, C. E. Brion, J. P. D. Cook, I. E. McCarthy, and E. Weigold, *Chem. Phys.* **91**, 373 (1984).
- 305 M. S. Banna, B. H. McQuaide, R. Malutzki, and V. Schmidt, *J. Chem. Phys.* **84**, 4739 (1986).
- 306 T. Moitra, A. C. Paul, P. Decleva, H. Koch, and S. Coriani, *Phys. Chem. Chem. Phys.* **24**, 8329 (2022).
- 307 M. S. Banna and D. A. Shirley, *Chem. Phys. Lett.* **33**, 441 (1975).
- 308 M. S. Banna and D. A. Shirley, *J. Chem. Phys.* **63**, 4759 (1975).
- 309 A. J. Yench, M. C. A. Lopes, M. A. MacDonald, and G. C. King, *Chem. Phys. Lett.* **310**, 433 (1999).
- 310 S. J. Bintrim and T. C. Berkelbach, *J. Chem. Phys.* **154**, 041101 (2021).
- 311 E. Monino and P.-F. Loos, *J. Chem. Theory Comput.* **17**, 2852 (2021).
- 312 E. Monino and P.-F. Loos, *J. Chem. Phys.* **156**, 231101 (2022).
- 313 J. Tölle and G. K.-L. Chan, “Ab- g_{0w_0} : A practical g_{0w_0} method without frequency integration based on an auxiliary boson expansion,” (2023), [arXiv:2311.18304 \[physics.chem-ph\]](https://arxiv.org/abs/2311.18304).
- 314 C. J. C. Scott, O. J. Backhouse, and G. H. Booth, *J. Chem. Phys.* **158**, 124102 (2023).
- 315 P. Ring and P. Schuck, *The Nuclear Many-Body Problem* (Springer, 2004).
- 316 G. E. Scuseria, T. M. Henderson, and I. W. Bulik, *J. Chem. Phys.* **139**, 104113 (2013).
- 317 D. Peng, S. N. Steinmann, H. van Aggelen, and W. Yang, *J. Chem. Phys.* **139**, 104112 (2013).
- 318 T. C. Berkelbach, *J. Chem. Phys.* **149**, 041103 (2018).
- 319 A. B. Trofimov and J. Schirmer, *J. Chem. Phys.* **123**, 144115 (2005).
- 320 S. Banerjee and A. Y. Sokolov, *J. Chem. Phys.* **151**, 224112 (2019).
- 321 J. Schirmer, L. S. Cederbaum, and O. Walter, *Phys. Rev. A* **28**, 1237 (1983).
- 322 A. Y. Sokolov, *J. Chem. Phys.* **149**, 204113 (2018).
- 323 D. L. Hildenbrand, *Int. J. Mass Spect. Ion Phys.* **7**, 255 (1971).
- 324 S. Svensson, M. Carlsson-Göthe, L. Karlsson, A. Nilsson, N. Mårtensson, and U. Gelius, *Phys. Scr.* **44**, 184 (1991).
- 325 P. Baltzer, M. Larsson, L. Karlsson, B. Wannberg, and M. Carlsson-Göthe, *Phys. Rev. A* **46**, 5545 (1992).
- 326 A. W. Potts and T. A. Williams, *J. Electron Spectrosc. Relat. Phenom.* **3**, 3 (1974).
- 327 L. Åsbrink and C. Fridh, *Phys. Scr.* **9**, 338 (1974).
- 328 L. Åsbrink, C. Fridh, E. Lindholm, and K. Codling, *Phys. Scr.* **10**, 183 (1974).
- 329 M. S. Banna and D. A. Shirley, *J. Electron Spectrosc. Relat. Phenom.* **8**, 255 (1976).
- 330 P. R. Norton, R. L. Tapping, H. P. Broida, J. W. Gadzuk, and B. J. Wacławski, *Chem. Phys. Lett.* **53**, 465 (1978).
- 331 S. R. Langhoff and C. W. Bauschlicher, Jr., *J. Chem. Phys.* **88**, 329 (1988).
- 332 R. C. Morrison and G. Liu, *J. Comp. Chem.* **13**, 1004 (1992).
- 333 A. K. Dutta, N. Vaval, and S. Pal, *J. Chem. Theory Comput.* **11**, 2461 (2015).
- 334 J. Berkowitz, C. H. Batson, and G. L. Goodman, *J. Chem. Phys.* **71**, 2624 (1979).
- 335 J. Bauschlicher, Charles W. and S. R. Langhoff, *J. Chem. Phys.* **87**, 2919 (1987).
- 336 M. L. Abrams and C. D. Sherrill, *J. Chem. Phys.* **121**, 9211 (2004).
- 337 C. D. Sherrill and P. Piecuch, *J. Chem. Phys.* **122**, 124104 (2005).
- 338 X. Li and J. Paldus, *Chem. Phys. Lett.* **431**, 179 (2006).
- 339 G. H. Booth, D. Cleland, A. J. W. Thom, and A. Alavi, *J. Chem. Phys.* **135**, 084104 (2011).
- 340 F. A. Evangelista, *J. Chem. Phys.* **134**, 224102 (2011).
- 341 S. Gulania, T.-C. Jagau, and A. I. Krylov, *Faraday Discuss.* **217**, 514 (2019).
- 342 A. Ammar, A. Marie, M. Rodríguez-Mayorga, H. G. A. Burton, and P.-F. Loos, “Can GW Handle Multireference Systems?” (2024), [arxiv:2401.03745](https://arxiv.org/abs/2401.03745).
- 343 K. Hamrin, G. Johansson, U. Gelius, C. Nordling, and K. Siegbahn, *Phys. Scr.* **1**, 277 (1970).
- 344 M. Patanen, K. J. Børve, J. A. Kettunen, S. Urpelainen, M. Huttula, H. Aksela, and S. Aksela, *J. Electron Spectrosc. Relat. Phenom.* **185**, 285 (2012).
- 345 Y. Zheng, C. E. Brion, M. J. Brunger, K. Zhao, A. M. Grisogono, S. Braidwood, E. Weigold, S. J. Chakravorty, E. R. Davidson, A. Sgamellotti, and W. von Niessen, *Chem. Phys.* **212**, 269 (1996).
- 346 D. C. Frost, S. T. Lee, and C. A. McDowell, *Chem. Phys. Lett.* **17**, 153 (1972).
- 347 N. Jonathan, A. Morris, M. Okuda, K. J. Ross, and D. J. Smith, *Faraday Discuss. Chem. Soc.* **54**, 48 (1972).
- 348 A. W. Potts and E. P. F. Lee, *Faraday Discuss. Chem. Soc.* **75**, 941 (1979).
- 349 P. Tomasello and W. von Niessen, *Mol. Phys.* **69**, 1043 (1990).
- 350 C. L. French, C. E. Brion, and E. R. Davidson, *Chem. Phys.* **122**, 247 (1988).

- ³⁵¹J. P. D. Cook, C. E. Brion, and A. Hamnett, *Chem. Phys.* **45**, 1 (1980).
- ³⁵²M. Y. Adam, C. Cauletti, and M. N. Piancastelli, *J. Electron Spectrosc. Relat. Phenom.* **42**, 1 (1987).
- ³⁵³D. M. Chipman, *J. Electron Spectrosc. Relat. Phenom.* **14**, 323 (1978).
- ³⁵⁴A. J. Yench, A. J. Cormack, R. J. Donovan, A. Hopkirk, and G. C. King, *Chem. Phys.* **238**, 109 (1998).
- ³⁵⁵M. Y. Adam, *Chem. Phys. Lett.* **128**, 280 (1986).
- ³⁵⁶S. Svensson, L. Karlsson, P. Baltzer, B. Wannberg, U. Gelius, and M. Y. Adam, *J. Chem. Phys.* **89**, 7193 (1988).
- ³⁵⁷D. Edvardsson, P. Baltzer, L. Karlsson, M. Lundqvist, and B. Wannberg, *J. Electron Spectrosc. Relat. Phenom.* **73**, 105 (1995).
- ³⁵⁸P.-M. Guyon, R. Spohr, W. A. Chupka, and J. Berkowitz, *J. Chem. Phys.* **65**, 1650 (1976).
- ³⁵⁹W. Domcke, L. S. Cederbaum, J. Schirmer, W. von Niessen, C. E. Brion, and K. H. Tan, *Chem. Phys.* **40**, 171 (1979).
- ³⁶⁰M. Hochlaf and J. H. D. Eland, *J. Chem. Phys.* **123**, 164314 (2005).
- ³⁶¹T. P. Fehlner and W. S. Koski, *J. Am. Chem. Soc.* **86**, 2733 (1964).
- ³⁶²J. H. Wilson and H. A. McGee, Jr., *J. Chem. Phys.* **46**, 1444 (1967).
- ³⁶³S. X. Tian, *J. Phys. Chem. A* **109**, 5471 (2005).
- ³⁶⁴G. Wälz, D. Usvyat, T. Korona, and M. Schütz, *J. Chem. Phys.* **144**, 084117 (2016).
- ³⁶⁵A. K. Dutta, N. Vaval, and S. Pal, *Int. J. Quant. Chem.* **118**, e25594 (2018).
- ³⁶⁶G. Pauley Paran, C. Utku, and T.-C. Jagau, *Phys. Chem. Chem. Phys.* **26**, 1809 (2024).
- ³⁶⁷D. Kánnár, A. Tajti, and P. G. Szalay, *J. Chem. Theory Comput.* **13**, 202 (2017).
- ³⁶⁸B. Kozma, A. Tajti, B. Demoulin, R. Izsák, M. Nooijen, and P. G. Szalay, *J. Chem. Theory Comput.* **16**, 4213 (2020).
- ³⁶⁹M. Patanen, A. R. Abid, S. T. Pratt, A. Kivimäki, A. B. Trofimov, A. D. Skitnevskaya, E. K. Grigorieva, E. V. Gromov, I. Powis, and D. M. P. Holland, *J. Chem. Phys.* **155**, 054304 (2021).
- ³⁷⁰C. Hättig, in *Response Theory and Molecular Properties (A Tribute to Jan Lindenberg and Poul Jørgensen)*, Advances in Quantum Chemistry, Vol. 50, edited by H. A. Jensen (Academic Press, 2005) pp. 37–60.
- ³⁷¹M. Govoni and G. Galli, *J. Chem. Theory Comput.* **14**, 1895 (2018).
- ³⁷²S. A. C. Clark, E. Weigold, C. E. Brion, E. R. Davidson, R. F. Frey, C. M. Boyle, W. von Niessen, and J. Schirmer, *Chem. Phys.* **134**, 229 (1989).
- ³⁷³A. Ferté, J. Palaudoux, F. Penent, H. Iwayama, E. Shigemasa, Y. Hikosaka, K. Soejima, K. Ito, P. Lablanquie, R. Taïeb, and S. Carniato, *J. Phys. Chem. Lett.* **11**, 4359 (2020).
- ³⁷⁴A. Ferté, F. Penent, J. Palaudoux, H. Iwayama, E. Shigemasa, Y. Hikosaka, K. Soejima, P. Lablanquie, R. Taïeb, and S. Carniato, *Phys. Chem. Chem. Phys.* **24**, 1131 (2022).